ORIGINAL PAPER



Mutations in the plant-conserved uL1m mitochondrial ribosomal protein significantly affect development, growth and abiotic stress tolerance in *Arabidopsis thaliana*

Emilio Núñez-Delegido 1 • Pablo Teruel-Elvira • Pedro Robles • Aitana Seller-Lozano 1 • David Domínguez-Espinosa 1 • Víctor Quesada 1 • David Domínguez-Espinosa 1 • Víctor Quesada 1 • David Domínguez-Espinosa 2 • Víctor Quesada 3 • David Domínguez-Espinosa 3 • Víctor Quesada 3 • David Domínguez-Espinosa 4 • David Domínguez-Espinosa 5 • David Do

Received: 12 October 2024 / Accepted: 10 January 2025 / Published online: 25 February 2025 © The Author(s) 2025

Abstract

Mitochondria ribosomes, or mitoribosomes, reflect the endosymbiotic origin of this organelle. Mitoribosomes are made up of RNAs and proteins (mitochondrial ribosomal proteins, MRPs). Considering the large amount of MRPs identified in plant mitoribosomes, the number of MRPs for which mutations producing mutant phenotypes have been hitherto reported is rather limited. Moreover, the contribution of plant mitoribosomes, and hence mitochondrial translation, to abiotic stress, is almost completely unknown. To advance knowledge about the role of mitochondrial translation in plant development and stress acclimation, we performed a thorough genetic and phenotypic analysis of the Arabidopsis mrpl1-1 and 3 mutants affected in the MRPL1 (MITOCHONDRIAL RIBOSOMAL PROTEIN L1) gene encoding MRP uL1m. Compared to the wild type, the mrpl1-1 and 3 mutants show delayed growth, small body size and smaller leaf palisade cells, although the morphology of chloroplasts and mitochondria is similar. We identified a novel MRPL1 mutant allele, mrpl1-2, that causes early seedling lethality, which reveals that Arabidopsis MRPL1 is an essential gene. Furthermore, the mrpl1 viable mutants are less responsive than the wild type to increased growth temperature, and are hypersensitive to antibiotics doxycycline and chloramphenicol, and also to salt, osmotic and ABA stress. In summary, impaired MRPL1 function severely hinders plant growth and development, likely by triggering retrograde signaling due to translational perturbation, and it enhances sensitivity to abiotic stress. Besides, our results support a role for mitochondria translation in acclimation to adverse environmental conditions. To our knowledge this is the first work to report an altered abiotic stress sensitivity phenotype due to mutations in a plant MRP gene.

Keywords Mitochondrial ribosomal protein \cdot *MRPL1* gene \cdot *Arabidopsis* \cdot Abiotic stress tolerance \cdot Plant growth and development

Introduction

Mitochondria have their own machinery for carrying out the synthesis of proteins encoded by the genome of the organelle: mitochondrial ribosomes (or mitoribosomes). They are composed of two subunits, one large and one small, consisting of ribosomal RNAs (rRNAs) and proteins. Today's

Emilio Núñez-Delegido and Pablo Teruel-Elvira have contributed equally.

∀íctor Quesada vquesada@umh.es

mitoribosomes originated from the ribosomes of the endosymbiont from which mitochondria derive, an ancestral α-proteobacterium related to present-day Rickettsia (Gray 1999). During evolution, the overwhelming majority of endosymbiont genes, including those for ribosomal proteins, were transferred to the host nuclear genome (Lang et al. 1999; Timmis et al. 2004). As a consequence, all the genes encoding mitochondrial ribosomal proteins (MRPs) in animals are nuclear, whereas some of these genes in plants and certain protists are still located in the mitochondrial genome (or mitogenome). Besides, their spatial arrangement sometimes resembles that existing in the ancestral bacterial operons from which they originate (Lang et al. 1999). Presentday mitoribosomes differ from their bacterial counterpart in many fundamental aspects. Along these lines, rRNA and



Instituto de Bioingeniería, Universidad Miguel Hernández, Campus de Elche, 03202 Elche, Spain

MRP composition differs from that of bacterial ribosomes, such as those of *Escherichia coli*. Furthermore, although all mitoribosomes have a common prokaryotic origin, their structure and composition substantially differ between different eukaryotic lineages (Amunts et al. 2015; Greber et al. 2015; Ramrath et al. 2018; Soufari et al. 2020).

Three-dimensional (3D) structures of bacterial and cytosolic ribosomes were obtained by X-ray crystallography several years ago (Clemons et al. 1999; Ben-Shem et al. 2011). However, the characterization and determination of the 3D structures of mitoribosomes, which are less abundant than their bacterial and cytosolic counterparts, have only been possible thanks to the development of the cryoelectron microscopy (cryo-EM) technique. Cryo-EM has revealed the composition and structure of mitoribosomes from animals, fungi, kinetoplasts, land plants, protozoa and unicellular photosynthetic algae (Amunts et al. 2015; Greber et al. 2015; Desai et al. 2017; Ramrath et al. 2018; Waltz et al. 2019, 2020, 2021; Tobiasson and Amunts 2020). These results highlight that, beyond a shared set of proteins that might have been present in the common ancestor of all mitoribosomes, different groups of eukaryotes independently recruited specific sets of proteins to make specialized ribosomes.

Plant growth and development require a high input of energy and metabolites. Mitochondria are responsible for providing energy to cells in the form of ATP, which allows them to carry out numerous metabolic processes. Therefore, the disruption of mitochondrial translation is expected to significantly affect organelle activity and, consequently, plant growth and development. In line with this, some examples are known in different plant species, mainly in Arabidopsis thaliana (hereafter Arabidopsis), of mutations in MRPs that disrupt growth and developmental processes, such as embryo formation, leaf morphogenesis or reproductive development, highlighting the important role of MRPs in all these processes (Robles and Quesada 2017). Along these lines, the Arabidopsis heart stopper (hes) mutant, which is affected in MRP uL18m, shows low proliferation of seed endosperm cells and arrested embryo development in the late globular stage (Zhang et al. 2015). In maize, the defective kernel44 (dek44) mutant affected in MRP bL9m shows small kernels with severe developmental delay and contains dead embryos (Qi et al. 2019). Other MRPs are involved in the formation of reproductive tissues. Accordingly, the Arabidopsis huellenlos-1 (hll-1) mutant, which is affected in the gene that encodes MRP uL14m, displays arrested ovule development before or immediately after the formation of the ovule teguments, or even after these teguments have started extending around the nucellus, as in hll-2. The hll-1 and hll-2 mutants also exhibit a smaller gynoecium than the wild type and a few ovules (Skinner et al. 2001). The Arabidopsis nuclear fusion defective 1 (nfd1) and nfd3 mutants,

which are respectively impaired in the genes encoding MRPs bL21m and uS11m, show altered fusion of polar nuclei during female gametophyte development (karyogamy). *nfd1* is also affected in karyogamy during fertilization and male gametophyte development (Portereiko et al. 2006).

Mutations have also been described in MRPs to affect leaf morphogenesis. Accordingly, the NCS3 (non-chromosomal stripe) mutant of maize shows sparsely developed tissue sectors in leaves and cobs due to a deletion produced by mitochondrial DNA rearrangement in the region containing the rps3 and rpl16 genes, which encode MRPs uS3M and uL16M, respectively (Hunt and Newton 1991). The RNAi-mediated silencing of the Arabidopsis nuclear gene encoding MRP uS10m significantly disrupts leaf morphology. This disruption occurs because reduced levels of uS10m alter the stoichiometric balance between the large and small mitoribosome subunits, thereby affecting the translation of mitochondrial genes (Majewski et al. 2009; Kwasniak et al. 2013). More recently, characterization of Arabidopsis mutant rps9m-3, has revealed a role for MRP uS9m during vegetative and reproductive development (Lu et al. 2020). Thus, rps9m-3 mutant exhibits a pleiotropic phenotype, characterized by abnormal development of male gametophytes, seeds and delayed germination. Furthermore, rps9m-3 main root and stem length, rosette diameter and silique size are small compared to the wild type (Lu et al. 2020).

Besides playing a key role in plant growth and development, mitochondria are also involved in metabolic processes required for cell adaptation to adverse environmental conditions (Pastore et al. 2007). Not surprisingly, the analysis of several mutants, mainly in Arabidopsis and rice, has revealed an association between mitochondrial function and plant acclimation to abiotic stress. Some of these mutants are affected in nuclear genes involved in organelle gene expression (OGE) in mitochondria and show altered responses to different abiotic stresses (reviewed in Leister et al. 2017). Thus the ppr96 (pentatricopeptide repeat protein96) mutants show reduced sensitivity to NaCl, abscisic acid (ABA) and oxidative stress caused by H₂O₂, while PPR96 expression increases in response to NaCl and oxidative stress (Liu et al. 2016). However, mutants abob (ABA-overly sensitive6; He et al. 2012), ppr40 (Zsigmond et al. 2008), pgn (ppr for germination on NaCl; Laluk et al. 2011), ahg11 (ABA hypersensitive germination11; Murayama et al. 2012), slg1 (slow growth1; Yuan and Liu 2012) and slo2 (slow growth2; Zhu et al. 2014) are all hypersensitive to ABA, salinity and osmotic stress during germination and early seedling growth (reviewed in Robles and Quesada 2019). Most of these mutants show changes in endogenous reactive oxygen species (ROS) levels due to altered mitochondrial function as a consequence of defects in the RNA editing of the mitochondrial transcripts that encode different subunits of oxidative phosphorylation (OXPHOS) complexes (e.g.



ahg11, slg1 and slo2) (Yuan and Liu 2012; Murayama et al. 2012; Zhu et al. 2014), altered splicing regulation of mitochondrial genes encoding subunits of OXPHOS Complex I (e.g. abo6) (He et al. 2012) or reduced ubiqinol-cytochrome c oxidoreductase activity of Complex III (e.g. ppr40) (Zsigmond et al. 2008). In line with this, the transgenic Arabidopsis plants that overexpress PPR40 display increased tolerance to salinity in association with lowering H_2O_2 levels and with decreased lipid peroxidation (Zsigmond et al. 2012).

Despite all the above-described mutant phenotypes, considering that 93 MRPs have been identified in the *Arabidopsis* mitoribosome, 49 and 44 in the large and small subunits, respectively (Waltz et al. 2019), the number of MRPs for which mutations producing mutant phenotypes have been reported is rather limited. Furthermore, consequences of abiotic stress on plant mitochondrial translation, the final stage of gene expression in this organelle, are almost completely unknown. To our knowledge, no plant MRP-affected mutant that displays an altered response to abiotic stress has been hitherto reported. In contrast, several mutants that are affected in nuclear genes encoding plastid ribosomal proteins and exhibiting abiotic stress phenotypes have been described (reviewed in Robles and Quesada 2022).

Wang and Auwerx (2017) found that mitochondrial translation stress in the mrpl1-1 (mitochondrial ribosomal protein 11-1) and mrp11-3 mutants, which are affected in the MRPL1 gene that encodes the mitochondrial ribosomal protein L1 (uL1m), leads to proteotoxic stress and activates the mitochondrial unfolded protein response (UPR^{mt}) to restore proteostasis in the organelle. In addition, Li et al. (2024) very recently reported that the mrpl1-3 mutant shows enhanced resistance to biotic stress through the induction of jasmonic acid (JA) accumulation and signaling. Notwithstanding, a detailed phenotypic analysis of the mrpl1-1 and 3 mutants is lacking. Therefore, we considered it worthwhile performing a thorough characterization of the phenotype of these mutants and identifying new mrpl1 mutant alleles to improve our understanding of MRPL1 function and, by extension, of MRPs during plant development. Furthermore, the eventual involvement of MRPL1 in plant acclimation to abiotic stresses has also been investigated in this work.

Results

Identification and genetic characterization of T-DNA lines affected in the MRPL1 gene

In a search for insertional mutants affected in nuclear genes encoding *Arabidopsis* MRPs, the *Salk_014201* and *Salk_206492* lines yielded individuals with a small body size compared to the wild-type Col-0. The phenotypic differences between the Col-0, *Salk_014201* and

Salk 206492 individuals are evident early on (Fig. 1A–I). The gene affected in both T-DNA lines, AT2G42710 (MRPL1), encodes the uL1m protein of the large subunit of the mitoribosome according to TAIR (https://www. Arabidopsis.org/locus?key=31744) and the SUBA Protein Subcellular Localisation Database (https://suba.live/subaapp/factsheet.html?id=AT2G42710). The small size of the Salk 014201 and Salk 206492 plants has been previously reported (Wang and Auwerx 2017; Li et al. 2024). The information available in the SIGnAL database (http:// signal.Salk.edu/cgi-bin/tdnaexpress) shows that T-DNAs are inserted into the first intron and the fifth exon of the AT2G42710 gene in the Salk_014201 and Salk_206492 lines, respectively. We confirmed this by PCR genotyping and Sanger sequencing by using different oligonucleotide combinations (Table S1 and Figure S1). We respectively named the Salk 014201 and Salk 206492 lines mrpl1-1 and *mrpl1-3*, according to Wang and Auwerx (2017).

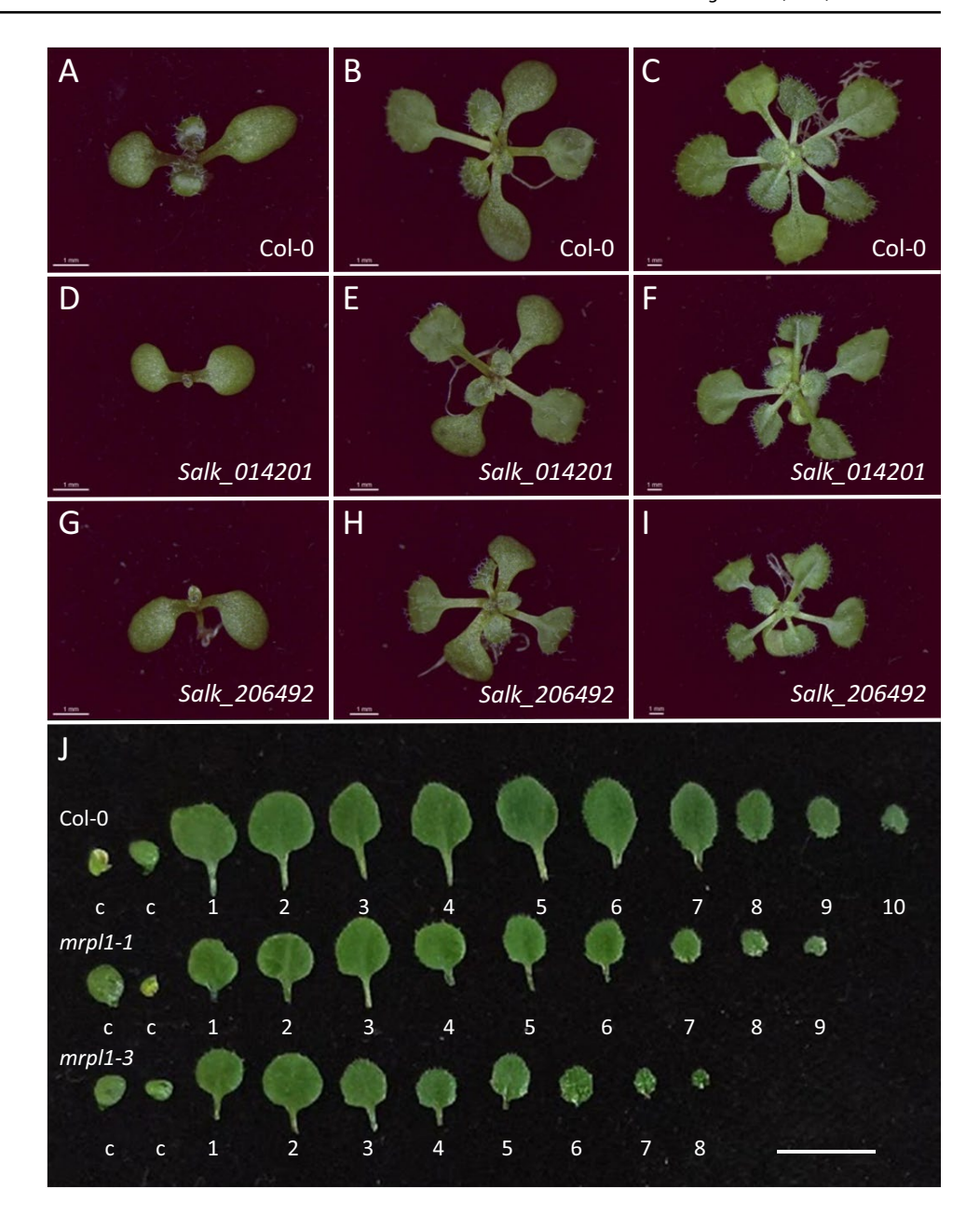
The mrpl1-1 and mrpl1-3 mutants were backcrossed to Col-0 to eliminate putative additional unwanted insertions and to ascertain the inheritance pattern of mutations. The F_2 progenies displayed a 3:1 wild-type:mutant (180:59) segregation ratio for mrpl1-1 ($\chi^2=0.026$; p=0.986) and mrpl1-3 (182:61) ($\chi^2=0.001$; p=0.970), which denotes that the mutant phenotypes are monogenic and recessive. We established homozygous F_3 populations for both insertional lines from selfed F_2 mutant individuals and genotyped them by PCR and Sanger sequencing. F_3 seeds from the homozygous mutant plants were collected and used to perform the experiments described ahead.

To study the expression of the MRPL1 gene in the mrpl1 mutants and Col-0, RNA was extracted from 14-das (days after stratification) plants, reverse-transcribed and PCR-amplified using different primer combinations (Table S1 and Figure S2A). No amplification of mrpl1 cDNA mutants was detected with F1 + R1 (in mrpl1-1) or F3 + R3 (in mrpl1-3) oligonucleotides (Figure S2B, C), suggesting that T-DNA, or at least part of it, must be present in the MRPL1 transcripts in the mutants. In contrast, MRPL1 transcripts were detected upstream of the insertion in mrpl1-3 (with primers F1 and R1) and downstream of the T-DNA in *mrpl1-1* (with primers F3 and R3; Figure S2). Nevertheless, if these mutant transcripts are translated, the T-DNA insertion could introduce premature stop codons, leading to early termination of translation (Wang et al. 2008).

We analyzed *MRPL1* expression using TraVa, a database of *Arabidopsis* gene expression profiles based on RNA-seq results (http://travadb.org/). We detected *MRPL1* transcripts in all the tissue and organ samples available in TraVa, with the highest levels in seeds after being soaked in water for 1 day, in the shoot apical meristem in the vegetative stage, and also after floral transition (Table S2). This shows that



Fig. 1 Morphological phenotypes of the seedlings and vegetative rosettes of Salk_014201, Salk_206492 and wild-type Col-0. Representative images of the wild-type Col-0 (A-C), Salk_014201(D-F) and Salk_206492 (G-I) plants at 9 (A, D, G), 14 (B, E, H) and 20 (C, F, I) days after stratification (das). (J) Cotyledons (c) and the first to the tenth (1-10)rosette leaves collected at 20 das from Col-0 and the mrpl1-1 and mrpl1-3 mutants. Scale bars represent 1 mm (A-I) and 1 cm (J)



MRPL1 is primarily expressed in very early plant life cycle stages and in regions of high cell proliferation.

We identified a third T-DNA line, $Salk_083354$, putatively carrying an insertion in the MRPL1 gene according to SIGnAL. The $Salk_083354$ T₃ plants did not show any obvious phenotypic alterations. However, we found T₄ seedlings that did not survive beyond 5 das, which fitted a 3:1 (220 wild-type:68 lethal mutants) segregation ratio (χ^2 =0.3379; P=0.8445) (Figure S3A-C), something expected if the lethal phenotype was due to a single recessive mutation. To confirm that the $Salk_083354$ line carried a new mutant allele of the MRPL1 gene, we crossed a phenotypically wild-type putatively heterozygous T₄ $Salk_083354$ plant (which segregated wild-type and lethal seedlings in the T₅ generation)

with an mrpl1-1 mutant plant. We found that eight and nine F_1 plants displayed the wild-type and mutant phenotype, respectively, which was expected from the non complementation between a heterozygote and a homozygote affected by mutations in the same gene. Consequently, we named the $Salk_083354$ line mrpl1-2. The putative F_1 compound heterozygote plants mrpl1-1/mrpl1-2 are not lethal, but exhibit an identical mutant phenotype to that of the homozygous mrpl1-1/mrpl1-1 individuals, which suggests dominance of the mrpl1-1 allele over mrpl1-2. To confirm that the F_1 individuals displaying a mutant phenotype were indeed mrpl1-1/mrpl1-2 plants, we studied their F_2 progenies. As expected, we found that phenotypically mutant mrpl1-1 and early seedling lethal individuals fitted a 3:1 (Mrpl1-1:lethal)



segregation ratio in all cases. Genotyping alleles *mrpl1-1* and *mrpl1-2* in the F₂ non-lethal mutant individuals allowed us to identify plants *mrpl1-1/mrpl1-2* (Figure S4B-D). We determined the location of T-DNA in the *mrpl1-2* allele by Sanger sequencing the PCR products from gDNA of plants F₂ *mrpl1-1/mrpl1-2*. The T-DNA in *mrpl1-2* is inserted into intron 8, 13 nucleotides downstream of the 3' end of exon 8 of the *MRLP1* gene (Figure S4A). These results demonstrate that we have identified a new mutant allele of the *MRPL1* gene, *mrpl1-2*, which causes lethality very early during *Arabidopsis* seedling development.

Bioinformatics analysis of the L1p/L10e ribosomal protein family

The Arabidopsis uL1m protein has a predicted length of 415 amino acids and a molecular weight of 45.8 kDa. It belongs to the L1p/L10e ribosomal protein family (L1 in prokaryotes and L10 in eukaryotes) according to TAIR (https://www.Arabidopsis.org/). We searched for paralogous Arabidopsis proteins to uL1m using their amino acid sequence as a query and the online tool BLASTP from TAIR. We identified a single uL1m homologous protein, the product of the AT3G63490 gene, which shows 38% identity with uL1m and is probably located in chloroplasts according to the information available in TAIR and SUBA (https://suba.live/suba-app/factsheet.html?id=AT2G4 2710; Hooper et al. 2014). We investigated the conservation of the Arabidopsis uL1m protein in both prokaryotes and photosynthetic eukaryote species. To this end, we first identified the L1 ribosomal proteins of three bacterial species: Escherichia coli, Thermus thermophilus and Bacillus subtilis. With the NCBI BLASTP tool (https:// blast.ncbi.nlm.nih.gov/Blast.cgi), we determined the levels of identity of uL1m with its orthologs in these bacterial species: 40.79% (E. coli), 41.44% (T. thermophilus) and 40.27% (B. subtilis). A multiple alignment of the amino acid sequences of the ribosomal proteins encoded by the Arabidopsis genes MPRL1 and AT3G63490 and the L1s of E. coli, T. thermophilus and B. subtilis revealed that the conserved region is primarily confined to the L1p/L10e domain, whose presence we have previously determined using SMART (http://smart.embl-heidelberg.de/) (Fig. 2). Interestingly, Arabidopsis proteins are larger than their bacterial homologs. This is due mainly to the presence of transit peptides to mitochondria (MRPL1) and chloroplasts (AT3G63490 protein), which are respectively 39 and 70 amino acids long, which we identified using the TargetP v2.0 subcellular localization predictor algorithm (Emanuelsson et al. 2000) (Fig. 2). This is consistent with the endosymbiotic origin of mitochondria and chloroplasts, and with the subsequent gene transfer from these organelles to the cell nucleus (Bogorad 1975). A slight increase in the number of amino acids was also found at the C-terminal ends of the *Arabidopsis* L1 proteins compared to their bacterial homologs.

We employed the information available in the PLAZA v3.0 database to identify the uL1m orthologous proteins in other photosynthetic species. PLAZA v3.0 is a webbased resource that centralizes the sequences and annotations produced by different genome sequencing initiatives of photosynthetic organisms, which makes it a very useful tool for comparative genomics studies (Proost et al. 2015). In line with this, 31 uL1m orthologous proteins in 29 plant species (Table S3) were identified. Twentyseven species harbor a single gene encoding a protein with an L1p/L10e domain, while Malus domestica and Glycine max respectively have three and two genes each (Table S3). Orthologous uL1m proteins were identified in monocots, dicots, and bryophyte Physcomitrella patens, which indicates that their origin predates the separation of vascular and non vascular plants. The number of exons in the genes encoding uL1m orthologous proteins is highly conserved (10 in most of them), but we also identified genes with a smaller number [nine in Amborella trichopoda (ATR00130G00370) and Malus domestica (MD09G023090), and four in Prunus persica (PPE003G10820)] or higher (12 in Malus domestica MD00G001330 and MD00G195850) (Table S3). The number of amino acids ranged from 248 (Lotus japonicus LJ3G021300) to 535 (Malus domestica MD00G001330 and MD00G195850), although almost all of them were about 350 amino acids long. The proteins with the highest level of identity with uL1m were encoded by AL4G30100 (Arabidopsis lyrata) and CRU004G24240 (Capsella rubella), and with 95.71% and 91.47% identity, respectively (Table S3). These results were expected seeing that Arabidopsis lyrata, Capsella rubella and Arabidopsis belong to the Brassicaceae or Cruciferae family. The proteins with the lowest identity with Arabidopsis uL1m were MD00G001330 and MD00G195850 (Malus domestica) and PPE003G10820 (Prunus persica), with 41.65%, 41.87% and 43.02% identity, respectively. A multiple alignment with the amino acid sequences of plant uL1m orthologous proteins revealed a high conservation level, mainly in the region of the L1p/L10e domain (Figure S5A). TargetP v2.0 (Emanuelsson et al. 2000) predicted mitochondrial localization for nearly all the uL1m orthologous proteins, except for RC29428G00070 (Ricinus communis), LJ3G021300 (Lotus japonicus) and VV12G03000 (Vitis vinifera) (Table S3). The Weblogo tool showed that the first amino acids (~16) of the N-terminal transit peptide of the putatively mitochondrial uL1m orthologs were highly conserved and largely hydrophobic (Figure S5B).



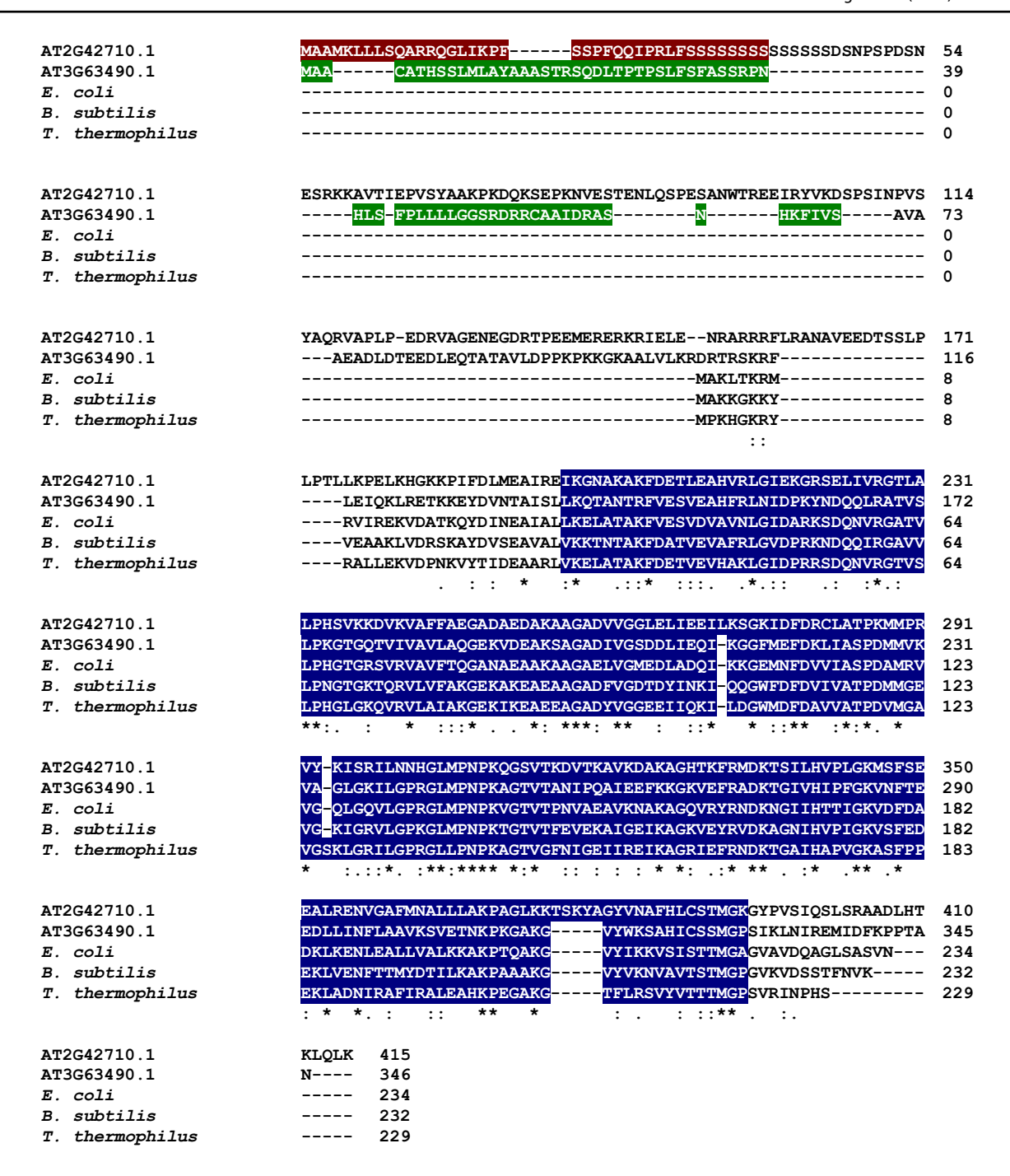


Fig. 2 Multiple alignment of the amino acid sequences of the L1 ribosomal proteins. Multiple alignment of the amino acid sequences of the L1 proteins from *Arabidopsis thaliana* (AT2G42710 and AT3G63490), *Escherichia coli (E. coli*; UniProt accession number P0A7L0), *Thermus thermophilus* (*T. thermophilus*; UniProt accession number Q5SLP7) and *Bacillus subtilis* (*B. subtilis*; UniProt accession number Q06797) are shown. The residues shaded in red and green

correspond to the transit peptides to mitochondria and chloroplast, respectively, predicted using TargetP v2.0 (Emanuelsson et al. 2000). The residues shaded in blue denote the L1p/L10e domain. The alignment was obtained using CLUSTAL OMEGA (Madeira et al., 2019). Asterisks (*) indicate the residues conserved across all the sequences. Two dots (:) and one dot (.) denotes the residues sharing strong and weak chemical properties, respectively



Phenotypic characterization of the *mrpl1-1* and 3 mutants

In order to phenotypically characterize *mrpl1* mutants, we studied in detail in viable mutants *mrpl1-1*, *mrpl1-3* and Col-0: germination, seedling establishment (cotyledon greening and expansion), the appearance of leaves in the rosette and flowering time. We also analyzed in Col-0 and the *mrpl1* mutants several body parameters, such as rosette area, length of the main root, primary stems, siliques and hypocotyl, and the number of seeds per silique.

The *mrpl1* mutants showed delayed germination. Thus, at 2 das, 60% and 20% of the wild-type and mutant seeds germinated, respectively, whereas the germination values of the mutants and the wild type were similar from 3 das onward (Figure S6A). For seedling establishment, a substantial delay was observed in the *mrpl1* mutants compared to Col-0. Thus at 4 das, seedling establishment was achieved for 76% of the Col-0 seeds, while no mutant seeds yielded seedlings with green expanded cotyledons. At 5 das, 96%, 53% and 56% of the Col-0, *mrpl1-1* and *mrpl1-3* seeds respectively yielded seedlings with green expanded cotyledons. From 6 das onward, the Col-0 and mutant seeds had values of ~ 100% (Figure S6B).

We collected and photographed cotyledons and all the rosette leaves of Col-0 and the *mrpl1* mutants at 20 das to compare their size and morphology. There were fewer and smaller leaves in the mutants than in Col-0, but no significant morphological differences. Thus 10 leaves could be

collected from Col-0 vs. 9 and 8 from *mrpl1-1* and *mrpl1-3*, respectively, with the mutant leaves being clearly smaller than those of the wild type (Fig. 1J). This indicates that rosette leaf appearance is delayed in *mrpl1* compared to the Col-0 plants.

The Col-0 plants flower earlier than the mrpl1 mutants (Figure S7A). Thus at 27 das, 25% of the Col-0 individuals bolted compared to only 2% and 4% of mrpl1-1 and mrpl1-3, respectively. These percentages were 77%, 25% and 27% for Col-0, mrpl1-1 and mrpl1-3 at 31 das (Figure S7B). This suggests that stunting likely delayed bolting in the mrpl1 mutants and led to shorter plants (Figure S8A). We did not observe any appreciable differences between either the mrpl1 and Col-0 flowers or between the mrpl1 and Col-0 green siliques (Figure S8B, C). For each mrpl1 mutant and Col-0, 10 green and 10 dry siliques were dissected. No morphological differences were found between the green or dry seeds of Col-0 and the *mrpl1* mutants (Figure S8D, E). Quantification of the length of green siliques and the number of seeds per silique after dissection confirmed lack of significant differences between Col-0 and the mrpl1 mutants (Table 1).

The small size of the *mrpl1-1* and 3 plants compared to Col-0 was confirmed by measuring the rosette area, fresh and dry weights, and the main root length for both genotypes. In all cases, the mutant values were always significantly lower than in the wild type (Table 1). Besides, the length of the primary stems of the Col-0 and *mrpl1-1* and 3 plants was significantly shorter in the mutants than in Col-0

Table 1 Morphometric analysis of the *mrpl1* mutants

Body parameters	Genotype			
	das	Col-0	mrpl1-1	mrpl1-3
Rosette area	14	41.9 ± 14.3	13.9 ± 6.3*	14.2±5.8*
Fresh weight	14	20.6 ± 4.2	$6.8 \pm 1.0 *$	$8.5 \pm 1.4*$
		50.2 ± 11.9^{a}	$13.9 \pm 3.0^{a,*}$	$14.8 \pm 2.6^{a,*}$
Dry weight	14	2.4 ± 0.5	$1.1 \pm 0.3*$	$1.2 \pm 0.3*$
		4.5 ± 1.1^{a}	$1.5 \pm 0.3^{a,*}$	$1.7 \pm 0.4^{a,*}$
Root length	14	71.8 ± 9.2	$23.4 \pm 1.6*$	$22.4 \pm 4.2*$
Hypocotyl length ^b	11	15.7 ± 0.8	15.5 ± 1.4	15.8 ± 1.0
Primary stem length	54	85.0 ± 22.2	$18.7 \pm 17.7*$	$23.0 \pm 21.0*$
	60	188.5 ± 27.0	$74.0 \pm 40.8 *$	$102.0 \pm 42.2*$
	67	311.5 ± 36.1	$161.5 \pm 63.2*$	$238.3 \pm 65.9*$
Silique length	54	17.0 ± 0.9	16.7 ± 1.2	17.1 ± 1.1
Number of seeds per silique	54	48.8 ± 6.6	48.3 ± 5.8	50.7 ± 5.9

Values are the mean of at least 15 measurements ± standard deviation (SD) per genotype. Area, length and weight values are indicated as mm², mm and mg, respectively

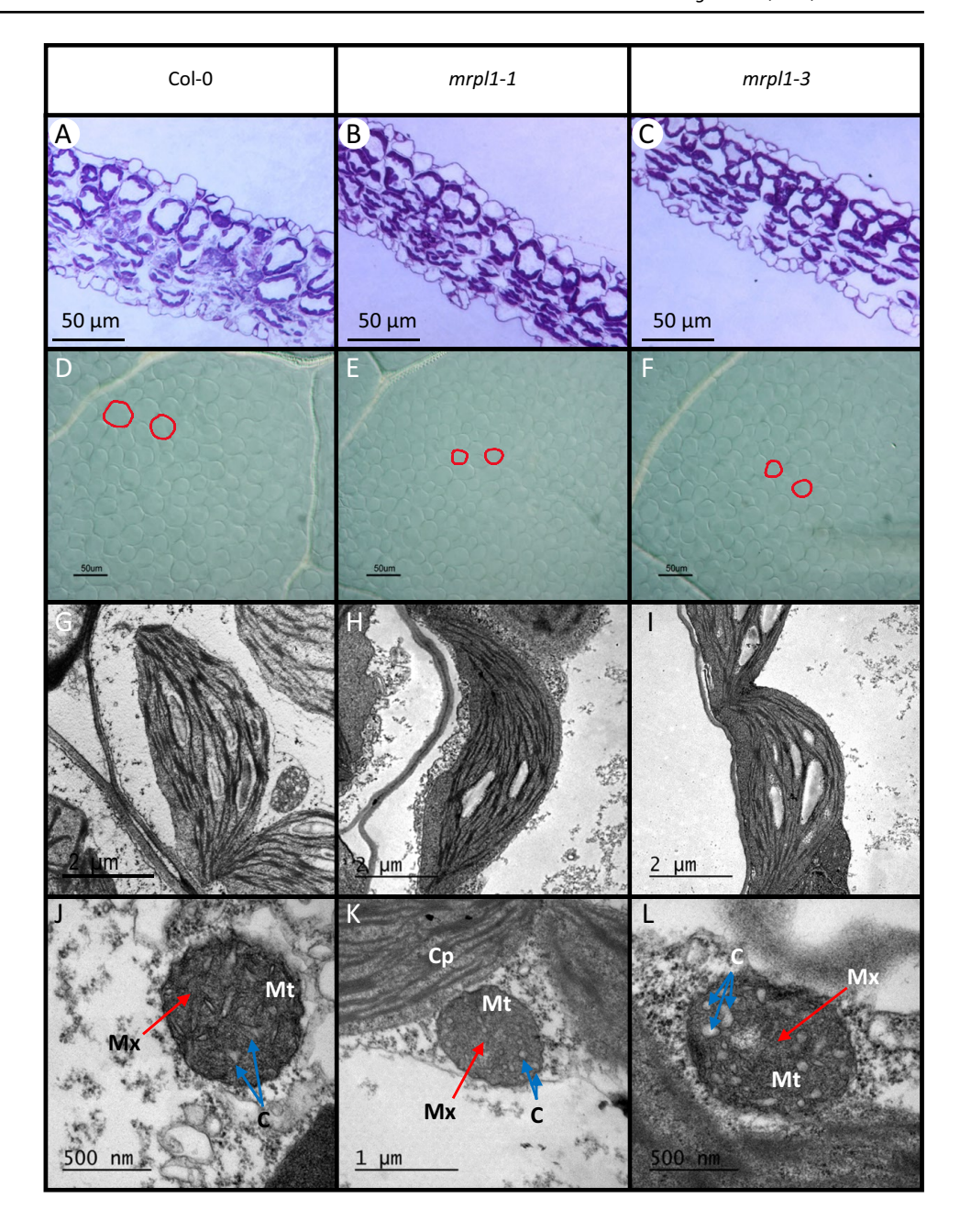
^{*}Values were significantly different (Student's t-test, P < 0.01) from those of the wild type (Col-0). das: days after stratification



 $^{^{}m a}$ These values correspond to plants grown at 28 $^{\circ}$ C. The remaining values in the table were obtained from plants grown at 20 $^{\circ}$ C

^bSeedlings grown in the dark

Fig. 3 Ultrastructure of the leaves in Col-0 and the mrpl1 mutants. Representative images of the transverse leaf sections (A-C) and palisade cells by interference contrast microscopy (D-F) of the third or fourth vegetative leaves of Col-0 (\mathbf{A}, \mathbf{D}) and the mrpl1-1 (**B**, **E**) and mrpl1-3 (**C**, **F**) mutants. The perimeter of some palisade cells is highlighted in red (D-F). Transmission electron micrographs of the chloroplasts (G-I) and mitochondria (J-L) of Col-0 (G, J) and the mrpl1-1 (H, K) and mrpl1-3 (I, L) mutants. Photographs were taken at 21 das. Red and blue arrows point to the mitochondrial matrix and cristae, respectively. Mt: mitochondria, Cp: chloroplast, Mx: matrix, C: cristae



at all the measured das (Table 1). No significant differences were found in hypocotyl length between the *mrpl1* and Col-0 individuals (Table 1).

Leaf ultrastructure of the mrpl1-1 and 3 mutants

Given the reduction in size of the *mrpl1* rosette leaves (Fig. 1J), we decided to investigate if the *mrpl1* mutations could affect the size of leaf mesophyll cells. To this end, we studied cross-sections of the third and fourth leaves of Col-0 and the mutant plants at 21 das. We found that palisade cells were apparently smaller than those of the wild type (Fig. 3A–C). To confirm this, the third and

fourth vegetative leaves from Col-0 and the *mrpl1* mutant plants were collected at 21 das, decolorized using chloral hydrate, and palisade cells were observed under an optical microscope with interdifferential contrast (Nomarski) (Fig. 3D–F). The *mrpl1-1* and 3 palisade cells were significantly smaller than those of the Col-0 leaves, as we confirmed by quantifying the mean area of cells: 686.6 ± 230.1 , 412.5 ± 134.7 and 592.7 ± 197.7 µm² in Col-0, *mrpl1-1* and *mrpl1-3*, respectively (Table S4).

To further explore the effect of defective *MRPL1* on leaf development, chloroplast and mitochondrion morphology was studied by transmission electron microscopy of leaf mesophyll cells. *mrpl1* chloroplasts and mitochondria



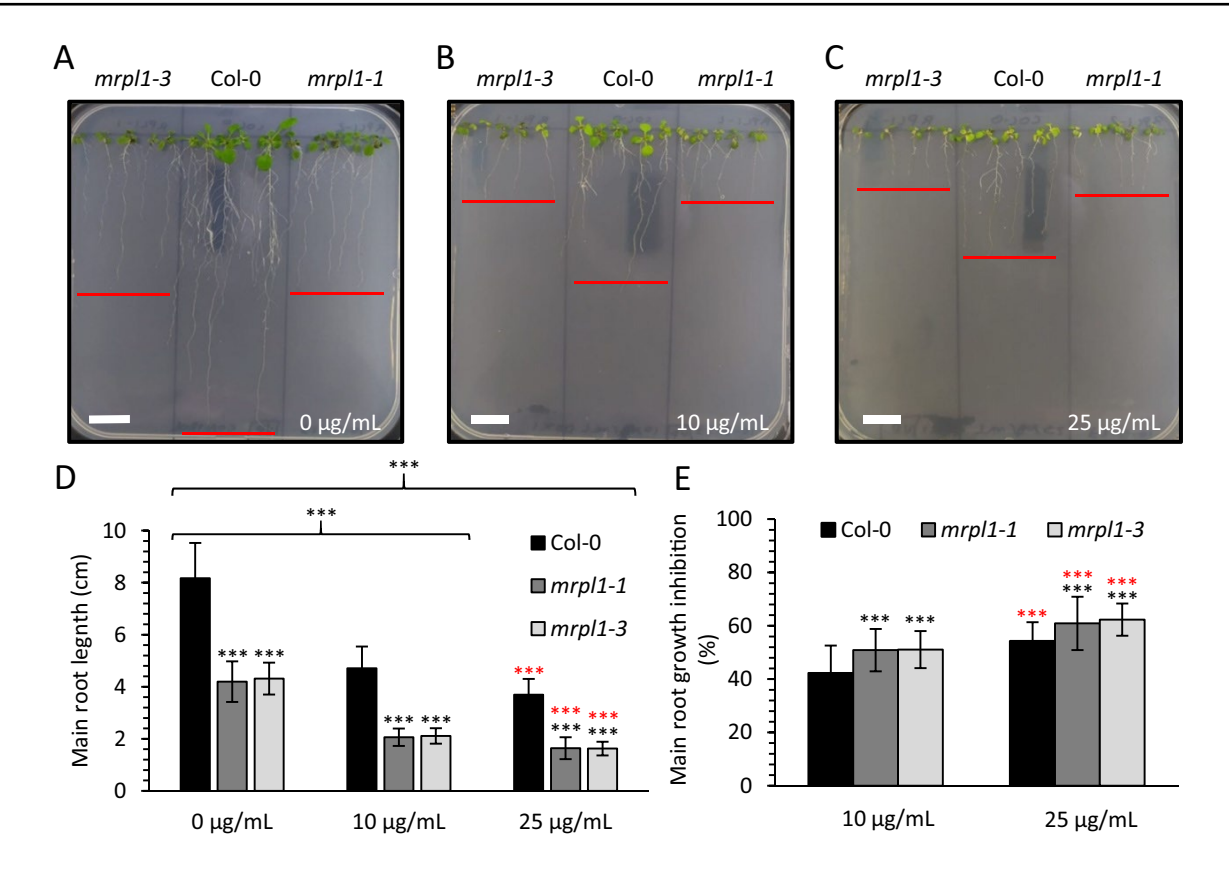


Fig. 4 Effect of doxycycline on the *mrpl1* mutants. Images correspond to the wild-type Col-0 and *mrpl1-1* and *mrpl1-3* mutant individuals grown vertically in Petri dishes at 13 das in either non supplemented (**A**) or growth media supplemented with 10 μ g/mL (**B**) or 25 μ g/mL (**C**) of doxycycline. Values correspond to the mean \pm SD of the main root length of plants Col-0, *mrpl1-1* and *mrlp1-3*. Each value represents the average of two independent experiments with at least 18 plants per genotype and experiment (**D**). Values correspond to the mean percentage \pm SD of root length inhibition of plants transferred 8 das to growth media supplemented with either 10 μ g/mL or 25 μ g/mL of doxycycline, referred to those of plants of the same

genotype, which were transferred to non supplemented media. Five days after transfer (13 das), the main root length was determined per plant to evaluate their tolerance to the antibiotic (E). Scale bar represents 1 cm (A–C). Red lines indicate the position of the root apical meristem of the main root. Asterisks denote statistically significant differences (***P<0.001) using the Student's t test. Black asterisks represent significant differences in relation to Col-0 and between the plants grown in the absence or presence of doxycycline. Red asterisks refer to statistically significant differences between the plants of the same genotype grown in 10 µg/mL and 25 µg/mL doxycycline

were similar in size and morphology to those of Col-0 (Fig. 3G–L). Nevertheless, we observed that the *mrpl1-1* mitochondria, usually displayed lower matrix density (i.e. less electron dense) and apparently fewer cristae compared to the Col-0 mitochondria (Fig. 3J–L).

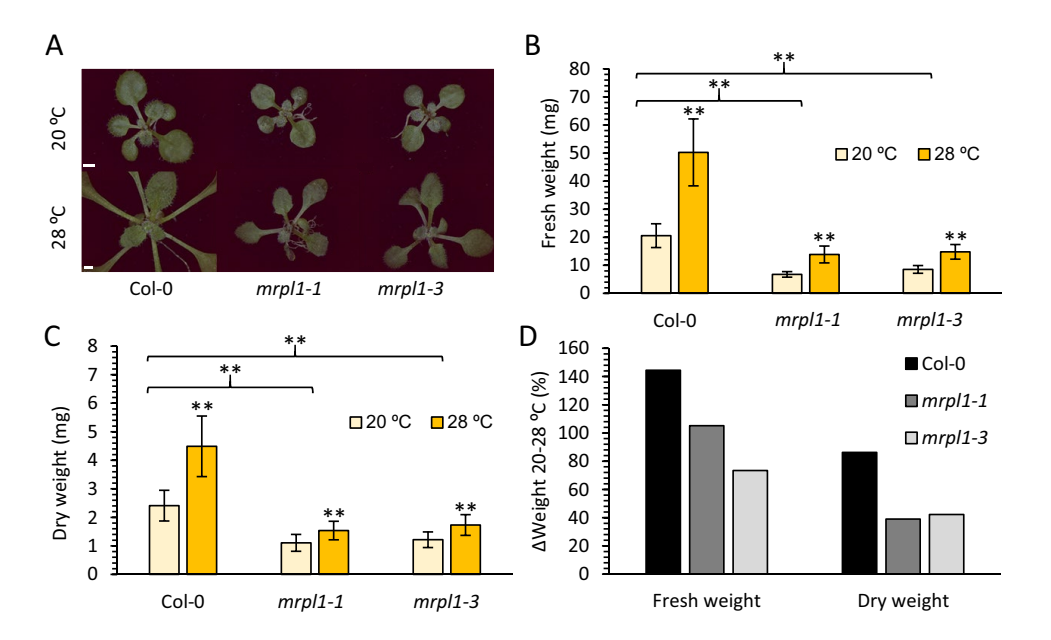
Sensitivity of the *mrpl1-1* and 3 mutants to doxycycline and chloramphenicol

Antibiotic doxycycline inhibits translation of the proteins encoded by mitochondrial DNA, but not by nuclear DNA (Clark-Walker and Linnane 1966). The *mrpl1* mutants exhibit a mitonuclear protein imbalance that causes proteotoxic stress in mitochondria (Wang and Auwerx 2017). Hence we decided to investigate the effect that chemical interference of mitochondrial translation using doxycycline could have on the phenotype of the *mrpl1*

mutants to check whether the mrpl1 individuals could be more sensitized than Col-0 to this antibiotic. To this end, mutants Col-0, mrpl1-1 and mrpl1-3 were grown in MS-agar medium without doxycycline. At 8 das, the individuals of each genotype were transferred to MS-agar medium supplemented with 10 µg/mL or 25 µg/mL doxycycline. As a control, we transferred the same number of seedlings of each genotype to non supplemented growth medium. Petri dishes were arranged vertically in the culture chamber and, 5 days later, we quantified the main root length of the transferred plants. Doxycycline significantly reduced the main root length of the mutant and wild-type individuals compared to the plants of the same genotype grown in the non supplemented control medium. This reduction was slightly more pronounced in 25 µg/mL than in 10 µg/mL of antibiotic (Fig. 4A–D). We quantified the inhibitory effect of doxycycline by normalizing the



Fig. 5 Effect of culture temperature on the *mrpl1* mutants. Representative rosettes of the Col-0 and mrpl1-1 and mrpl1-3 mutant individuals at 14 das (A). Values correspond to the mean \pm SD of the fresh (B) and dry (C) weights (mg) of at least 20 plants per genotype grown at 20 °C or 28 °C. The percentage of increase in the fresh and dry weights of the Col-0 and mrpl1 individuals grown at 28 °C in relation to the plants of the same genotypes grown at 20 °C is plotted (D). Data were obtained at 14 das. Asterisks indicate significant differences (**P<0.01) using a Student's t-test. Scale bars: 1 mm



root length of the mutant and wild-type individuals grown in the presence of the antibiotic by that of the individuals of the same genotype grown in the control medium. The percentage inhibition of the main root length at 10 µg/mL doxycycline in plants mrpl1-1 and mrpl1-3 was 50.89% and 51.08%, respectively, and was 42.43% in Col-0 (Fig. 4E). Increasing the doxycycline concentration to 25 µg/mL enhanced the percentage of inhibition, which reached 60.91%, 62.32% and 54.2% in mrpl1-1, mrpl1-3 and Col-0, respectively (Fig. 4B). Consistently with this, the mrpl1 mutants were also significantly more sensitive than the wild type to antibiotic chloramphenicol, which also inhibits mitoribosomal translation (Figure S9A-C). We quantified the inhibitory effect of chloramphenicol by normalizing the root length of the mutant and wild-type individuals grown in the presence of 7.5 µM chloramphenicol by that of the individuals of the same genotype grown under the control conditions. The percentage of inhibition of root growth in mrpl1-1 and mrpl1-3 was 76.6% and 78.25%, respectively, and was 53% in Col-0 (Figure S9D).

Taken together, these results reveal that the *mrpl1* mutants are more sensitive than Col-0 to doxycycline and chloramphenicol, which falls in line with the altered mitochondrial function in the *mrpl1* mutants due to translational stress.

mrpl1 mutants exhibit a reduced response to increased growth temperature

We decided to investigate whether stunted *mrpl1* plants growth could be affected when grown at 28 °C vs. 20 °C, being the last one the temperature that we normally use. Culture at 28 °C led to increased growth and, hence, a bigger

size of the Col-0, mrpl1-1 and 3 individuals, although these differences were much more marked in Col-0 than in the mutants (Fig. 5A). To quantify these differences, the fresh and dry weights of the 14-das wild-type and mutant plants grown at 28 °C and 20 °C were determined. As expected, the mrpl1 mutants showed significantly lower fresh and dry weights than the wild type at 20 °C (Fig. 5B, C). When grown at 28 °C, the fresh and dry weights of both the mrpl1 mutants and Col-0 plants significantly increased compared to the values obtained at 20 °C (Fig. 5B, C), which aligns with these plants' enlarged size when grown at 28 °C vs. 20 °C (Fig. 5A). To ascertain whether impaired MRPL1 function could affect the increase in weight due to growth at 28 °C, we determined the increases in fresh and dry weights at 28 °C vs. 20 °C, and expressed them as percentages (Fig. 5D). We found that 28 °C enhanced the fresh and dry weights respectively of Col-0 by 144.5% and 86.3%, of mrpl1-1 by 105.1% and 39% and of mrpl1-3 by 73.4% and 42.25% (Fig. 5D). These results are consistent with the lesser increase in rosette size observed in mrpl1 compared to Col-0 when plants were grown at 28 °C vs. 20 °C (Fig. 5A), and demonstrate that the mrpl1 plants are less responsive than Col-0 to a rise in culture temperature.

mrpl1 mutants are hypersensitive to salt, mannitol and ABA stresses

Impaired function of the nuclear genes involved in OGE can significantly alter plant abiotic stress tolerance (reviewed in Quesada 2016; Leister et al. 2017; Robles and Quesada 2019; Wobbe 2020). Therefore, we set out to study whether the *Arabidopsis* uL1m protein might be involved in abiotic stress response. To this end, we decided to analyze the



MRPL1 promoter to identify stress-related *cis*-elements as well as to investigate the sensitivity of mutants *mrpl1-1* and 3 to different adverse environmental conditions and *MRPL1* expression in response to salt, mannitol and ABA stress.

To achieve the first objective, the ~ 1.5-kb sequences located upstream of the transcription start sites of the MRPL1 gene were analyzed using the online tools Plant-Care (http://bioinformatics.psb.ugent.be/webtools/plantcare/ html/; Lescot et al. 2002) and PLACE (https://www.dna. affrc.go.jp/PLACE/?action=newplace; Higo et al. 1999). Of the identified regulatory elements, we found that several were involved in the response to environmental stimuli, such as light (AE-box, GATA-motif or MRE), drought (MBS), salinity (GT1GMSCAM4) or low temperature (LTRE) (Table S5). We also identified the *cis*-elements required for etiolation-induced expression ACGTATERD1 and ABRE-LATERD1, or those involved in the response to phytohormones like ABA (ABRE), salicylic acid (as-1), auxin (TGA-element and NTBBF1ARROLB), ethylene (RAV), gibberellins (GARE) or cytokines (ARR1) (Table S5). Therefore, these results indicate that the MRPL1 promoter region harbors *cis*-elements involved in regulating its expression in response to different stresses (e.g. salinity) and phytohormones (e.g. ABA). To investigate the tolerance of the mrpl1 mutants to abiotic stress, Col-0 and the mrpl1 mutants were sown in MS-agar media supplemented with 150 mM NaCl or 350 mM mannitol, which respectively caused ionic and osmotic stress, and we examined germination and seedling establishment. Under the control conditions, germination, and principally seedling establishment, were delayed in the mrpl1 mutants compared to Col-0 (Fig. 6A, B) according to the results we previously obtained (see above). The mrpl1 mutants were significantly more sensitive than Col-0 to 150 mM NaCl during germination and seedling establishment, although mrpl1-1 exhibited greater sensitivity than mrpl1-3 (Fig. 6C, D). In line with this, at 5 das nearly 100% of the Col-0 seeds had germinated vs. only 58% and 76% of mrpl1-1 and mrpl1-3, respectively (Fig. 6C). For seedling establishment, the differences between Col-0 and the mrpl1 mutants were more evident. Thus the mrpl1 mutants did not reach the maximum seedling establishment value until 14 das, with 52% and 66% for mrpl1-1 and mrpl1-3 respectively, which were significantly lower values than those obtained for Col-0 (96%) (Fig. 6D).

In response to 350 mM mannitol, differences between the *mrpl1* mutants and Col-0 were less marked than in salt stress. Once again, the *mrpl1-1* mutant was more sensitive than *mrpl1-3* or Col-0 during germination and seedling establishment (Fig. 6E, F). Thus at 5 das, 97%, 53% and 84% respectively of the Col-0, *mrpl1-1* and *mrpl1-3* seeds germinated (Fig. 6E). The largest differences in seedling establishment between Col-0 and the *mrpl1* mutants appeared at 8 das, when 40% of the Col-0 seedlings displayed green

expanded cotyledons compared to 5% and 7% of *mrpl1-1* and *mrpl1-3*, respectively (Fig. 6E). At 12 das, Col-0 and the *mrpl1* mutants had the highest seedling establishment values, which remained unchanged (Fig. 6D).

The ABA phytohormone performs a crucial function in plant acclimation to adverse environmental conditions (Christmann et al. 2006). Several of the Arabidopsis mutants affected in proteins involved in OGE (including translation) also show altered sensitivity to abiotic stress and ABA (reviewed in Leister et al. 2017; Robles and Quesada 2019). Therefore, we decided to study the response to ABA of the mrpl1 mutants during germination and seedling establishment by growing them in MS-agar medium supplemented with 0.5 µM or 3 µM of this phytohormone. ABA sensitivity of the mrpl1 mutants was more evident in 3 than in 0.5 µM ABA although significant differences between Col-0 and mrpl1 mutants were also observed in the last condition (Fig. 7A–E). At 3 µM ABA concentration, 82%, 19% and 25% of the Col-0, mrpl1-1 and mrpl1-3 seeds had respectively germinated at 5 das, and these percentages had increased to 88%, 36% and 50% for Col-0, mrpl1-1 and mrpl1-3 at 6 das, respectively, (Fig. 7A, E). ABA reduced seedling establishment, and the mrpl1 mutants were more sensitive than Col-0. The differences were more marked from 9 to 14 das in 3 µM ABA (Fig. 7B, F). As with mannitol and NaCl, the *mrpl1-1* mutant was always more sensitive to ABA than mrpl1-3 (Fig. 7C-F).

To quantify the effect of salinity, osmotic stress and ABA on Col-0 and the mrpl1 mutants, the germination and seedling establishment percentages of all three genotypes grown in the presence of NaCl, mannitol or ABA were normalized by the percentage corresponding to the same genotype in the control media (Table S6). Hence the lower the value obtained, the stronger the effect of stress, and conversely. We found that NaCl, mannitol and ABA delayed germination and seedlings appearance with green expanded cotyledons in Col-0 and the mrpl1 mutants because they yielded values below 100% in almost all the assays. However, this delay more severely affected the mrpl1 mutants (especially mrpl1-1) than Col-0 (Table S6). Differences between Col-0 and the mrpl1 mutants became more evident during seedling establishment, because mutants yielded noticeably lower values than those of Col-0 throughout the 14 das (Table S6).

In order to investigate whether *MRPL1* expression could be modified by exposing the Col-0 plants to abiotic stress and/or to ABA, we analyzed by RT-qPCR the transcript levels of this gene in response to NaCl and ABA in Col-0 seedlings. To this end, we used the cDNA retrotranscribed from the total RNA extracted from the 10-das Col-0 seedlings grown in media supplemented, or not, with 100 mM NaCl or 1.5 μ M ABA as a template in qPCR amplifications. We previously demonstrated that these conditions significantly delay Col-0 germination and growth (Robles et al.



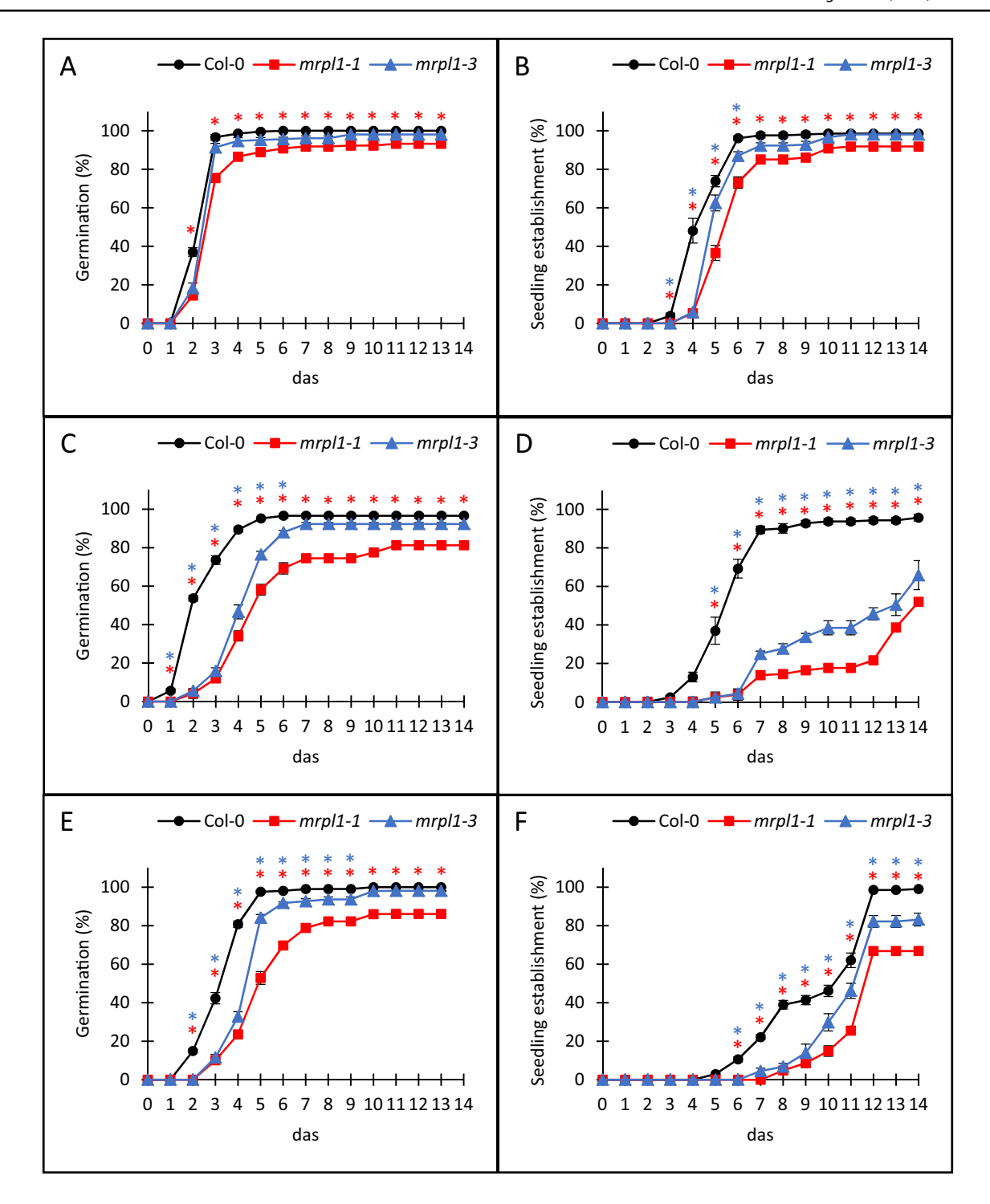


Fig. 6 Effects of NaCl and mannitol on germination and seedling establishment in the mrpl1 mutants. Each value corresponds to the mean \pm SD of the percentage of germination (**A**, **C**, **E**) and seedlings with green and expanded cotyledons (seedling establishment) (**B**, **D**, **F**) in growth media either not supplemented (**A**, **B**) or supplemented with 150 mM NaCl (**C**, **D**) or 350 mM mannitol (**E**, **F**), for four replicates of at least 50 seeds each per genotype. Seeds were consid-

ered germinated when radicle emergence through the seed testa was observed. Asterisks indicate statistically significant difference of germination and seedling establishment percentages of each mutant with respect to Col-0 in a two-sample z-test of proportions (*P<0.01). Red and blue asterisks indicate significant differences between mrpl1-1 and Col-0, and between mrpl1-3 and Col-0, respectively. das: days after stratification



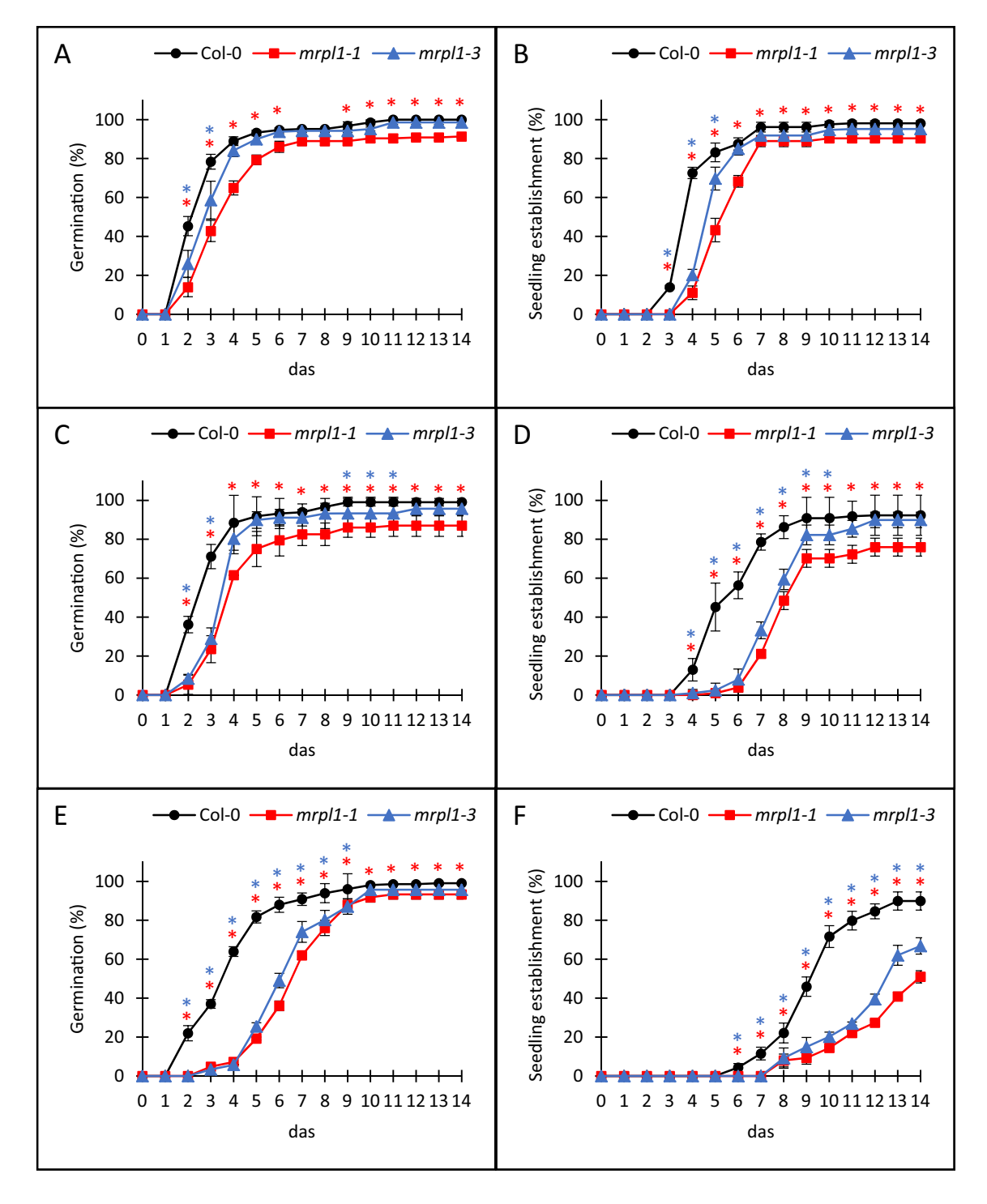


Fig. 7 Effects of ABA on germination and seedling establishment in the *mrpl1* mutants. Each value corresponds to the mean \pm SD of the percentage of germination (**A**, **C**, **E**) and seedling establishment (**B**, **D**, **F**) in growth media either not supplemented (**A**, **B**) or supplemented with 0.5 μ M (**C**, **D**) or 3 μ M (E, F) ABA, for four replicates of at least 50 seeds each per genotype. Asterisks indicate statistically

significant difference of germination and seedling establishment percentages of each mutant with respect to Col-0 in a two-sample z-test of proportions (*P<0.01). Red and blue asterisks indicate significant differences between mrpl1-1 and Col-0, and between mrpl1-3 and Col-0, respectively. das: days after stratification

2018a; Lidón-Soto et al. 2020). As controls, we included genes *RD29A* (*RESPONSIVE TO DESICCATION 29A*) and *COR15B* (*COLD-REGULATED 15B*) that are induced

by exposure to salinity, cold and ABA (Yamaguchi-Shinozaki and Shinozaki 2006; Lidón-Soto et al. 2020). Genes *COR15B* and *MRPL1* were significantly up-regulated in



response to 100 mM NaCl, although *MRPL1* expression (1.40 \pm 0.25; $p = 1.89 \times 10^{-3}$) was much lower than that of *COR15B* (3.6 \pm 1.15; $p = 4.11 \times 10^{-5}$). *RD29A* was significantly up-regulated (17.87 \pm 5.36; $p = 4.11 \times 10^{-5}$) and *MRPL1* was significantly down-regulated (0.43 \pm 0.12; $p = 4.11 \times 10^{-5}$) by ABA.

Taken together, our results demonstrate that *mrpl1* mutants exhibit enhanced sensitivity to salt stress and, to a lesser extent, osmotic stress induced by mannitol. Furthermore, *mrpl1* mutants display hypersensitivity to ABA, particularly during seedling establishment. Consistently, our findings also reveal that *MRPL1* expression is influenced by both abiotic stress and ABA.

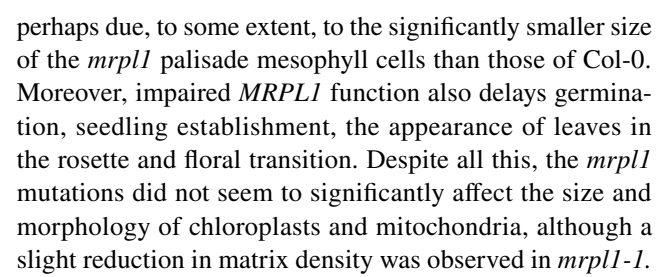
Discussion

Arabidopsis mrpl1 mutants are defective in vegetative growth and development

Proper ribosomes functioning is essential for the correct translation of the information contained in mRNA molecules. Notwithstanding, to date works reporting effects in plants of mutations in MRPs are scarce, except for those that affect reproductive development (reviewed in Robles and Quesada 2017). Furthermore, the molecular mechanisms by which MRPs modulate plant growth and development, as well as the contribution of mitochondrial ribosomes and, hence, translation, to abiotic stress acclimation are largely unknown.

In the work reported here, we used mutants mrpl1-1 and *mrpl1-3* to investigate the function of MRP uL1m in growth, development and acclimation to abiotic stress. Mutants mrpl1-1 and mrpl1-3 were backcrossed to Col-0 and the analysis of F₂ populations confirmed that both mutant phenotypes were due to single recessive mutations. We detected by sqRT-PCR MRPL1 transcripts downstream (in mrpl1-1) and upstream (in mrpl1-3) of the corresponding insertion. If these mutant transcripts are translated, the T-DNA insertion could likely introduce premature stop codons, potentially leading to truncated and chimeric proteins, lacking amino acids in their C-terminal regions and probably including some divergent amino acids, translated from the T-DNA insert (Figure S10). Nevertheless, the viability of mprl1-1 and 3 mutants suggests that they are hypomorphic rather than null alleles, and that mrpl1-1 and 3 aberrant proteins may still retain some function, as previously reported for other Arabidopsis T-DNA mutants yielding truncated and chimeric proteins (Hricová et al. 2006; Robles et al. 2012, 2015, 2018a, 2018b).

Rosette area, and fresh and dry weights, were significantly lower in *mrpl1-1* and *mrpl1-3* compared to Col-0



A reduction in mitochondrial respiration and the accumulation of the mitochondrial COXII protein in mutants mrpl1-1 and mrpl1-3 compared to Col-0 has been reported, and similar results have been obtained when applying doxycycline, a classic inhibitor of mitochondrial translation, to wild-type plants (Wang and Auwerx 2017). Hence lower levels of respiratory activity and proteotoxic stress caused by perturbed translation in mitochondria would negatively affect mrpl1 mutant growth. In line with this, the mrpl1-1 and mrpl1-3 individuals were more sensitive than Col-0 to doxycycline and chloramphenicol, which is consistent with mitochondrial stress in mutants. Mitochondrial proteotoxic stress triggers one of the retrograde signaling responses, the mitochondrial unfolded protein (UPR^{mt}) response, which leads to the activation of hormonal signaling to restore mitochondrial proteostasis (Wang and Auwerx 2017). The recent work by Li et al. (2024) revealed a key role for JA in this retrograde response because the mrpl1-3 mutation induces JA production, which contributes to plant growth repression in the mutant.

An increase in culture temperature can modify the phenotype of mutant plants affected in nuclear genes that encode mitochondrial proteins. Thus the Arabidopsis mterf22 (mitochondrial transcription termination factor 22) mutants impaired in mitochondrial protein mTERF22 exhibit a wildtype phenotype when grown at the usual growth temperature of 20 °C, but show defects when raised at 28 °C (Shevtsov et al. 2018). Culture at 28 °C vs. 20 °C enhanced the growth and size of the mrpl1 and Col-0 individuals. However, this increase was significantly greater in Col-0 than in the mrpl1 plants, which implies that the mrpl1 mutants are less responsive than Col-0 to a rise in culture temperature. Therefore, mitochondrial translation stress also hindered the response to enhanced growth temperature. Moreover, MRPL1 gene activity could be especially sensitive to a higher culture temperature, and maybe also to heat stress. Along these lines, a relation between plant mitochondrial activity and thermotolerance has been previously described because the shot1 (suppressor of hot1-4 1) mutants of Arabidopsis, which are affected in the nuclear gene that encodes the mitochondrial protein mTERF27, exhibited an altered response to heat (Kim et al. 2012).

A defective *MRPL1* function neither modifies the final size of siliques nor affects plant fertility. Likewise, the morphology of flowers and seeds did not alter in the



mrpl1-1 and mrpl1-3 individuals, which suggests that the uL1m protein is not required for their correct development, at least not under our growth conditions. Plant mutants defective in MRPs have been previously described, and like mutants mrpl1-1 and mrpl1-3, stunted growth was the most conspicuous trait (reviewed in Colas des Francs-Small and Small 2014). Unlike mrpl1 individuals however, a disruption of mitochondrial function in plants often results in additional phenotypic alterations such as in Arabidopsis and maize mutants appr6 (Arabidopsis pentatricopeptide repeat protein 6) and mppr6 respectively, affected in the gene encoding MRP uS3m (Manavski et al. 2012) and rps9m-3 mutant impaired in the Arabidopsis uS9c MRP (Lu et al. 2020).

We identified a third insertional allele of the *MRPL1* gene, *mrpl1-2*, which causes early seedling lethality in homozygosis. This suggests that *mrpl1-2* is a null or very strongly hypomorphic allele of the *MRPL1* gene, maybe because the T-DNA insertion at the 3' end of the *MRPL1* gene could greatly destabilize *mrpl1-2* transcripts and/or because it would lead to a long aberrant chimeric mrpl1-2 protein (Figure S10) with greater probability of misfolding, or of being unable to access its proper place on the ribosome. Consistent with this, insertions toward the 3' end of a gene before the stop codon and leading to lethality, have been previously reported in *Arabidopsis* (Robertson et al. 2004; Raschke et al. 2007).

To our knowledge, no mutations have been reported in plant MRPs to cause early lethality in seedlings, unlike what happens with plastid ribosomal proteins (PRPs). In the latter case, several examples of rice and maize mutants affected in PRPs, and showing lethality in the seedling stage, have been reported (reviewed in Robles and Quesada 2022). Lack of mutants impaired in MRPs and displaying early seedling lethality contrasts with the numerous examples known for years of mutations in MRPs causing embryonic, ovule or gametophyte lethality (Robles and Quesada 2017). This shows that mitochondrial function is especially critical in these plant development stages. As mrpl1-2/+ plants do not produce aborted or morphologically abnormal seeds, lack of MRPL1 does not seems to affect embryonic and gametophytic development like mutations in other MRPs do, such as the null alleles of HES (Zhang et al. 2015), HLL (Skinner et al. 2001) and NFD1 and 3 (Portereiko et al. 2006). So we cannot rule out either the notion that mrpl1-2 is not completely null, nor the threshold of remaining MRPL1 activity is enough to successfully reach the seedling stage. It is noteworthy that the orthologous L1 protein of E. coli is not essential because viable mutants that lack this protein have been obtained. However, these mutants show greatly reduced growth given half the protein synthesis rate for their ribosomes in *in vitro* assays (Baba et al. 2006).

Our *in silico* analyses showed that uL1m was a conserved protein among not only the major taxonomic groups of plants, but also in bacteria. Moreover, the similar sizes of the L1 proteins identified in plants, their predicted mitochondrial location for almost all of them and the high conservation of the number of exons of the genes encoding them, all strongly suggest a common evolutionary ancestor gene likely present in the last common ancestor of vascular and non vascular plants.

Impaired MRPL1 function alters plant acclimation to abiotic stress

We found that mutants mrpl1-1 and mrpl1-3 were more sensitive than the wild type to salt, osmotic and ABA stress, mainly during seedling establishment. Enhanced sensitivity to ABA, salt and osmotic stress has been previously reported in other Arabidopsis mutants, such as ppr40 and abo6, which are affected, like mrpl1, in nuclear genes encoding mitochondrial proteins. These mutants show damage in the mitochondrial electron transport chain and accumulate ROS in their mitochondria at higher levels than in the wild type (Zsigmond et al. 2008; He et al. 2012). As abiotic stress and ABA bring about a rise in ROS levels, the increased sensitivity to abiotic stress of ppr40 and abo6 is likely due to the accumulation of excess ROS caused by damage to the electron transport chain. This would be more pronounced under adverse environmental conditions because plant detoxification systems would be insufficient to prevent their accumulation (Zsigmond et al. 2008; He et al. 2012). Therefore, as mitochondrial respiration and translation are impaired in *mrpl1* individuals (Wang and Auwerx 2017), this would lead to ROS accumulation, which would increase sensitivity to abiotic stress. In line with this, in response to doxycycline Wang and Auwerx (2017) found a transient oxidative stress burst in redox sensor plants, as well as the up-regulation of the AOX1a gene, a classic marker or retrograde signaling in mitochondria, whose induction occurs in response to many stressors to protect against excessive ROS (Millar et al. 2011). Interestingly, the *AOX1a* gene was also upregulated in mrpl1-1 and mrpl1-3, which supports ROS accumulation due to an impaired uL1m function (Wang and Auwerx 2017).

The only mutant defective in an organelle ribosomal protein that displays an altered response to salinity hitherto described is *Arabidopsis psrp2*, affected in chloroplast-specific protein cS22 that binds RNA and possesses RNA chaperone activity (Xu et al. 2013). Interestingly, uL1 is the largest protein from the 50S ribosomal subunit and in *E. coli* it binds to the 23S rRNA and displays RNA chaperone activity, according to InterPro database (https://www.ebi.ac.uk/interpro/). Considering the degree of conservation of *Arabidopsis* and *E. coli* uL1 proteins, we cannot rule out that



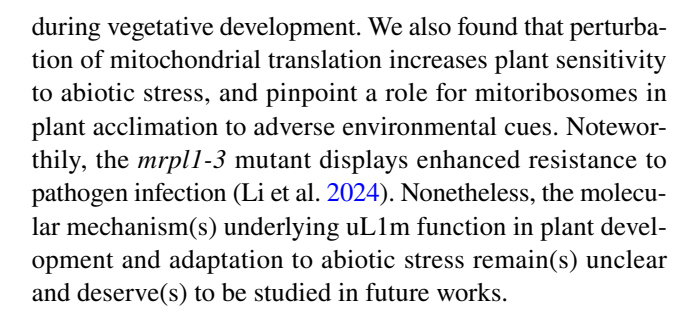
uL1m could also be able to bind RNA and act as an RNA chaperone. If so, this would suggest a relationship between translation, regulation of RNA metabolism in organelles and acclimation to abiotic stress conditions.

We found that MRPL1 gene expression was significantly increased and decreased in the Col-0 seedlings in the presence of moderate NaCl or ABA stress, respectively, compared to the non stressed seedlings. Several examples of Arabidopsis genes have been described which, like MRPL1, also show a differentially regulated expression by ABA and NaCl. Interestingly, some of these genes are also involved in OGE, such as those encoding the Arabidopsis nuclearencoded RNA polymerases targeted to plastids (RPOTp/ SCABRA3), plastids and mitochondria (RPOTmp) and mitochondria (RPOTm), or mTERF9, that promotes chloroplast ribosomal assembly and translation (Lidón-Soto et al. 2020; Méteignier et al. 2021). It is worth noting that loss-of-function mutants *mterf9* and *sca3* also exhibit growth retardation and an altered response to abiotic stress (Robles et al. 2015; Lidón-Soto et al. 2020). We previously demonstrated that growth in 100 mM NaCl impaired mitochondrial activity in the Col-0 seedlings and upregulated RPOTm expression via retrograde signaling from mitochondria to the nucleus, which could be interpreted as an attempt to provide energy and to maintain metabolism under stress (Lidón-Soto et al. 2020). This would be consistent with the herein described MRPL1 upregulation.

ROS function as signal transduction molecules by regulating different pathways during plant acclimation to stress (Choudhury et al. 2017). Therefore, we hypothesized that MRPL1 could be down-regulated by the retrograde signal/s from mitochondria to the nucleus produced in response to ABA, perhaps due to ROS accumulation promoted by ABA. Remarkably, OGE genes, including RPOTp, RPOTm and RPOTmp, were also down-regulated in Arabidopsis seedlings exposed to ABA (Danilova et al. 2018; Lidón-Soto et al. 2020). Hence our results revealed that the repressor effect of ABA on OGE also extends to the genes encoding MRPs, such as MRPL1. In line with the changes in MRPL1 transcript levels in response to abiotic stress, upstream of its translation initiation codon we identified several cissequences that are potentially involved in the regulation of its expression in response to different environmental stress conditions, as well as to phytohormones, including ABA.

Conclusions

Taken together, our findings demonstrate that unlike other mutations in plant MRPs, the impaired *Arabidopsis MRPL1* function does not cause a pleiotropic phenotype, but results in delayed growth and can lead to lethality very early on



Materials and methods

Plant materials and growth conditions

Crosses and plant cultures were performed as reported in Robles et al. (2012). The seeds of the Arabidopsis thaliana (L.) Heynh. wild-type accession Columbia-0 (Col-0) were obtained from the Nottingham Arabidopsis Stock Centre (NASC). The seeds of the T-DNA insertion lines Salk_014201, Salk_206492 and Salk_083354, all in a Col-0 genetic background, were provided by the NASC and are described on the SIGnAL website (Alonso et al. 2003; http:// signal.salk.edu). The rosette area of both mutants and wildtype plants was measured at 14 das using the ImageJ software (Schneider et al. 2012). Dry weight was measured in those plants that were oven-dried overnight at 55 °C. Flowering time was scored as the number of days upon bolting of plants grown under continuous light. A Student's t-test was applied to the obtained data at a significance level of 0.01. For the naming of mitochondrial ribosomal proteins, we have followed the nomenclature rules proposed by Scarpin et al. (2023).

Identification of the T-DNA insertions in the mutant lines

For the genotyping of the mutants, we extracted DNA from mutant plants T₄ and T₅, and from the F₂ segregating plants derived from backcrosses. DNA was PCR-amplified using the primers pairs designed by the T-DNA Primer Design (http://signal.salk.edu/tdnaprimers.2.html) tool, F1 and R1, F2 and R2, and F3 and R3, which hybridized with the genomic sequences flanking the insertions in the Salk_014201, Salk_206492 and Salk_083354 lines respectively. Primers F1, F2 and F3 were also used in combination with T-DNA specific primer LBa1 (Table S1).

Germination and growth sensitivity assays

For the germination assays, sowings were performed as described in Robles et al. (2012) on Petri dishes filled with GM agar medium [Murashige and Skoog (MS) containing



1% sucrose], supplemented with NaCl (150 mM), mannitol (350 mM) or ABA (0.5 or 3 µM). The seeds in which radicle emergence was observed were considered germinated, whereas seedling establishment was determined as the seedlings exhibiting green and fully expanded cotyledons. Seed germination and seedling establishment were scored from 1 to 14 das on Petri dishes, left at 20 ± 1 °C with 73 µmol·m⁻²·s⁻¹ of photons, and a two-sample z-test of proportions was applied to the percentage data obtained. For the chloramphenicol sensitivity assays, seeds were sown on Petri dishes filled with MS medium containing 1% sucrose and supplemented with 7.5 µM chloramphenicol, and arranged vertically in the culture chamber. The main root length was measured 14 days later. For the heat-sensitivity assays, plants Col-0, mrpl1-1 and mrpl1-3 were grown on Petri dishes at 28 ± 1 °C and 20 ± 1 °C for 14 das.

For the doxycycline sensitivity assays, seedlings were transferred to MS-agar medium non supplemented or supplemented with 10 or 25 $\mu g/mL$ doxycycline after 8 das on the MS control medium. As a control, the same number of seedlings of each genotype was transferred to non supplemented medium. Petri dishes were arranged vertically in the culture chamber and the main root length was measured 5 days later.

Computational analyses

Amino acid sequence comparisons and similarity searches were performed using BLAST (Altschul et al. 1990). The MRPL1 orthologs in photosynthetic species were identified with the PLAZA 3.0 database for comparative plant genomics (Proost et al. 2015). The subcellular localization of the analyzed proteins was predicted with Target P2.0 (Emanuelsson et al. 2007). The MRPL1 expression profiles in organs and developmental stages were obtained from TraVa (http:// travadb.org/; Klepikova et al. 2016). The identification of the putative abiotic stress cis-responsive elements present in the MRPL1 promoter was done by the PlantCare (http:// bioinformatics.psb.ugent.be/webtools/plantcare/html/; Lescot et al. 2002) and PLACE (https://www.dna.affrc.go. jp/PLACE/?action=newplace; Higo et al. 1999) online tools. The logo of the amino acid sequences was obtained using the WebLogo program (http://weblogo.berkeley.edu/).

Morphological and ultrastructural analyses

In order to visualize the internal structure of vegetative leaves, transverse sections were obtained from the third and fourth leaves of plants Col-0, *mrpl1-1* and *mrpl1-3* at 21 das. Leaf fragments were fixed, washed, postfixed, dehydrated and embedded in LR White resin as described in Hricová et al. (2006). The blocks containing leaf fragments were cut with a Reichert-Jung Ultracut E microtome to a thickness of

1.5 µm, stained with toluidine blue and mounted with Eukitt between a slide and coverslip to be visualized under a Leica DMRB microscope coupled to a Nikon DXM1200 digital camera. For visualizing palisade cells, plants were harvested at 21 das, and the third and fourth leaves were decolorized using chloral hydrate. Palisade cells were observed under an optical microscope using Nomarski differential interference contrast. The area of palisade cells was measured with the ImageJ software (Schneider et al. 2012). For transmission electron microscopy, the mutant and wild-type plant material was harvested at the same time of the day and prepared as described by Hricová et al., (2006). Samples were visualized under a Zeiss EM10C transmission electron microscope (Zeiss, http://www.zeis.com).

RNA extraction and semiquantitative RT-PCR (sqRT-PCR)

Total RNA was extracted using TRIsure (Bioline) from 80 mg of the Col-0, *mrpl1-1* and *mrpl1-3* 14-das seedlings. RNA was ethanol-precipitated and suspended in 40 μl of RNase-free water. DNA was removed using the TURBO DNAfree kit (Invitrogen) following the manufacturer's instructions. Two micrograms of each sample were reverse-transcribed with random hexamers/primers. The PCR amplifications of the first-strand cDNA were performed as described by Quesada et al. (1999). Then 1 μl of the cDNA solution was used for the sqRT-PCR amplifications. The housekeeping *ACTIN2* gene was employed as an internal control.

Quantitative RT-PCR (RT-qPCR)

Total RNA was extracted using TRIsure (Bioline) from 80 mg of 10-das Col-0 seedlings grown in the presence or absence of 100 mM NaCl or 1.5 µM ABA, in GM agar medium. RNA was resuspended in 40 µl of RNase-free water and DNA was removed using the TURBO DNAfree kit (Invitrogen) following the manufacturer's instructions. The cDNA preparations and qPCR amplifications were carried out in an ABI PRISM 7000 Sequence Detection System (Applied Biosystems), as described in Robles et al. (2012), using the oligonucleotides listed in Table S1. Each reaction mix of 20 µl contained 7.5 µl of the SYBR-Green/ROX qPCR Master Kit (Thermo Fisher), 0.4 μM of primers and 1 μl of cDNA solution. The relative quantification of the gene expression data was performed by the $2^{-\Delta\Delta CT}$ method as described in Robles et al. (2012). Each reaction was done in three replicates and three different biological replicates were used. The expression levels were normalized to the CT values obtained for the housekeeping ACTIN2 gene.



Supplementary Information The online version contains supplementary material available at https://doi.org/10.1007/s10725-025-01282-x.

Acknowledgements This work was supported by grants from the Vicerrectorado de Investigación of the Universidad Miguel Hernández de Elche to VQ and PR. The authors wish to thank Lidia Ortiz-Henarejos for her excellent assistance with the statistical analysis.

Author contributions VQ conceived and designed this paper. END, PTE, ASL and DDE conducted the experiments. The first draft of the manuscript was written by VQ. PR, END and PTE commented on previous versions of the manuscript and contributed to the discussion. All authors read and approved the final manuscript.

Funding Open Access funding provided thanks to the CRUE-CSIC agreement with Springer Nature. The authors declare that no funds, grants, or other support were received during the preparation of this manuscript.

Declarations

Competing interests The authors have no relevant financial or non-financial interests to disclose.

Open Access This article is licensed under a Creative Commons Attribution 4.0 International License, which permits use, sharing, adaptation, distribution and reproduction in any medium or format, as long as you give appropriate credit to the original author(s) and the source, provide a link to the Creative Commons licence, and indicate if changes were made. The images or other third party material in this article are included in the article's Creative Commons licence, unless indicated otherwise in a credit line to the material. If material is not included in the article's Creative Commons licence and your intended use is not permitted by statutory regulation or exceeds the permitted use, you will need to obtain permission directly from the copyright holder. To view a copy of this licence, visit http://creativecommons.org/licenses/by/4.0/.

References

- Alonso JM, Stepanova AN, Leisse TJ et al (2003) Genome-wide insertional mutagenesis of *Arabidopsis thaliana*. Science 301:653–657. https://doi.org/10.1126/science.1086391
- Altschul SF, Gish W, Miller W et al (1990) Basic local alignment search tool. J Mol Biol 215:403–410. https://doi.org/10.1016/S0022-2836(05)80360-2
- Amunts A, Brown A, Toots J et al (2015) The structure of the human mitochondrial ribosome. Science 348:95–98. https://doi.org/10. 1126/science.aaa1193
- Baba T, Ara T, Hasegawa M et al (2006) Construction of Escherichia coli K-12 in-frame, single-gene knockout mutants: the Keio collection. Mol Syst Biol. https://doi.org/10.1038/msb4100050
- Ben-Shem A, de Loubresse NG, Melnikov S et al (2011) The structure of the eukaryotic ribosome at 3.0 Å resolution. Science 334:1524–1529. https://doi.org/10.1126/science.1212642
- Bogorad L (1975) Eukaryotic Intracellular Relationships. In: Tzagoloff A (ed) Membrane Biogenesis: Mitochondria, Chloroplasts, and Bacteria. Springer, Boston, pp 201–245
- Choudhury FK, Rivero RM, Blumwald E, Mittler R (2017) Reactive oxygen species, abiotic stress and stress combination. Plant J 90:856–867. https://doi.org/10.1111/tpj.13299

- Christmann D, Himmelbach A, Yang Y, Tang Y, Grill EAM (2006) Integration of abscisic acid signalling into plant responses. Plant Biol 8:314–325. https://doi.org/10.1055/s-2006-924120
- Clark-Walker GD, Linnane AW (1966) Invivo differentiation of yeast cytoplasmic and mitochondrial protein synthesis with antibiotics. Biochem Biophys Res Commun 25:8–13
- Clemons WM, May JLC, Wimberly BT et al (1999) Structure of a bacterial 30S ribosomal subunit at 5.5 Å resolution. Nature 400:833–840. https://doi.org/10.1038/23631
- Colas des Francs-Small C, Small I (2014) Surrogate mutants for studying mitochondrially encoded functions. Biochimie 100:234–242. https://doi.org/10.1016/j.biochi.2013.08.019
- Danilova MN, Kudryakova NV, Andreeva AA et al (2018) Differential impact of heat stress on the expression of chloroplast-encoded genes. Plant Physiol Biochem 129:90–100. https://doi.org/10.1016/j.plaphy.2018.05.023
- Desai N, Brown A, Amunts A, Ramakrishnan V (2017) The structure of the yeast mitochondrial ribosome. Science 355:528–531. https://doi.org/10.1126/science.aal2415
- Emanuelsson O, Nielsen H, Brunak S, von Heijne G (2000) Predicting subcellular localization of proteins based on their N-terminal amino acid sequence. J Mol Biol 300:1005–1016. https://doi.org/10.1006/jmbi.2000.3903
- Emanuelsson O, Brunak S, von Heijne G, Nielsen H (2007) Locating proteins in the cell using TargetP, SignalP and related tools. Nat Protoc 2:953–971. https://doi.org/10.1038/nprot.2007.131
- Gray MW (1999) Evolution of organellar genomes. Curr Opin Genet Dev 9:678–687. https://doi.org/10.1016/S0959-437X(99)00030-1
- Greber BJ, Bieri P, Leibundgut M et al (2015) The complete structure of the 55S mammalian mitochondrial ribosome. Science 348:303–308. https://doi.org/10.1126/science.aaa3872
- He J, Duan Y, Hua D et al (2012) DEXH Box RNA helicase-mediated mitochondrial reactive oxygen species production in *Arabidop-sis* mediates crosstalk between abscisic acid and auxin signaling. Plant Cell 24:1815–1833. https://doi.org/10.1105/tpc.112.098707
- Higo K, Ugawa, Y, Iwamoto M, Korenaga, T (1999) Plant cis-acting regulatory DNA elements (PLACE) database: 1999. Nucleic Acids Res 27:297–300. https://doi.org/10.1093/nar/27.1.297
- Hooper CM, Tanz SK, Castleden IR et al (2014) SUBAcon: a consensus algorithm for unifying the subcellular localization data of the *Arabidopsis* proteome. Bioinformatics 30:3356–3364. https://doi.org/10.1093/bioinformatics/btu550
- Hricová A, Quesada V, Micol JL (2006) The SCABRA3 nuclear gene encodes the plastid RpoTp RNA polymerase, which is required for chloroplast biogenesis and mesophyll cell proliferation in Arabidopsis. Plant Physiol 141:942–956. https://doi.org/10.1104/pp. 106.080069
- Hunt MD, Newton KJ (1991) The NCS3 mutation: genetic evidence for the expression of ribosomal protein genes in Zea mays mitochondria. EMBO J 10:1045–1052. https://doi.org/10.1002/j.1460-2075.1991.tb08043.x
- Kim M, Lee U, Small I et al (2012) Mutations in an *Arabidopsis* mitochondrial transcription termination factor-related protein enhance thermotolerance in the absence of the major molecular chaperone HSP101. Plant Cell 24:3349–3365. https://doi.org/10.1105/tpc. 112.101006
- Klepikova AV, Kasianov AS, Gerasimov ES et al (2016) A high resolution map of the *Arabidopsis thaliana* developmental transcriptome based on RNA-seq profiling. Plant J 88:1058–1070. https://doi.org/10.1111/tpj.13312
- Kwasniak M, Majewski P, Skibior R et al (2013) Silencing of the nuclear RPS10 gene encoding mitochondrial ribosomal protein alters translation in *Arabidopsis* mitochondria. Plant Cell 25:1855–1867. https://doi.org/10.1105/tpc.113.111294
- Laluk K, AbuQamar S, Mengiste T (2011) The *Arabidopsis* mitochondria-localized pentatricopeptide repeat protein PGN functions in



- defense against necrotrophic fungi and abiotic stress tolerance. Plant Physiol 156:2053–2068. https://doi.org/10.1104/pp.111.177501
- Lang BF, Gray MW, Burger G (1999) Mitochondrial genome evolution and the origin of eukaryotes. Annu Rev Genet 33:351–397. https://doi.org/10.1146/annurev.genet.33.1.351
- Leister D, Wang L, Kleine T (2017) Organellar gene expression and acclimation of plants to environmental stress. Front Plant Sci. https://doi.org/10.3389/fpls.2017.00387
- Lescot M, Déhais P, Thijs G et al (2002) PlantCARE, a database of plant cis-acting regulatory elements and a portal to tools for in silico analysis of promoter sequences. Nucleic Acids Res 30:325–327. https://doi.org/10.1093/nar/30.1.325
- Li J, Yu G, Wang X et al (2024) Jasmonic acid plays an important role in mediating retrograde signaling under mitochondrial translational stress to balance plant growth and defense. Plant Commun. https://doi.org/10.1016/j.xplc.2024.101133
- Lidón-Soto A, Núñez-Delegido E, Pastor-Martínez I et al (2020) Arabidopsis plastid-RNA polymerase RPOTp Is involved in abiotic stress tolerance. Plants 9:834. https://doi.org/10.3390/plants9070834
- Liu J-M, Zhao J-Y, Lu P-P et al (2016) The E-subgroup pentatricopeptide repeat protein family in *Arabidopsis thaliana* and confirmation of the responsiveness *PPR96* to abiotic stresses. Front Plant Sci 7:1825. https://doi.org/10.3389/fpls.2016.01825
- Lu C, Xie Z, Yu F et al (2020) Mitochondrial ribosomal protein S9M is involved in male gametogenesis and seed development in *Arabi-dopsis*. Plant Biol 22:655–667. https://doi.org/10.1111/plb.13108
- Majewski P, Wołoszyńska M, Jańska H (2009) Developmentally early and late onset of Rps10 silencing in *Arabidopsis thaliana*: genetic and environmental regulation. J Exp Bot 60:1163–1178. https://doi.org/10.1093/jxb/ern362
- Madeira F, Mi Park Y, Lee J et al (2019) EMBL-EBI search and sequence analysis tools APIs in 2019. Nucleic Acids Res 47:636–641. https://doi.org/10.1093/nar/gkz268
- Manavski N, Guyon V, Meurer J et al (2012) An Essential pentatricopeptide repeat protein facilitates 5' maturation and translation initiation of rps3 mRNA in maize mitochondria. Plant Cell 24:3087–3105. https://doi.org/10.1105/tpc.112.099051
- Méteignier L-V, Ghandour R, Zimmerman A et al (2021) Arabidopsis mTERF9 protein promotes chloroplast ribosomal assembly and translation by establishing ribonucleoprotein interactions in vivo. Nucleic Acids Res 49:1114–1132. https://doi.org/10.1093/nar/ gkaa1244
- Millar AH, Whelan J, Soole KL, Day DA (2011) Organization and regulation of mitochondrial respiration in plants. Annu Rev Plant Biol 62:79–104. https://doi.org/10.1146/annurev-arpla nt-042110-103857
- Murayama M, Hayashi S, Nishimura N et al (2012) Isolation of *Arabidopsis ahg11*, a weak ABA hypersensitive mutant defective in *nad4* RNA editing. J Exp Bot 63:5301–5310. https://doi.org/10.1093/jxb/ers188
- Pastore D, Trono D, Laus MN et al (2007) Possible plant mitochondria involvement in cell adaptation to drought stress: a case study: durum wheat mitochondria. J Exp Bot 58:195–210. https://doi.org/10.1093/jxb/erl273
- Portereiko MF, Sandaklie-Nikolova L, Lloyd A et al (2006) NUCLEAR FUSION DEFECTIVE1 Encodes the *Arabidopsis* RPL21M protein and is required for karyogamy during female gametophyte development and fertilization. Plant Physiol 141:957–965. https:// doi.org/10.1104/pp.106.079319
- Proost S, Van Bel M, Vaneechoutte D et al (2015) PLAZA 3.0: an access point for plant comparative genomics. Nucleic Acids Res 43:974–981. https://doi.org/10.1093/nar/gku986
- Qi W, Lu L, Huang S, Song R (2019) Maize *Dek44* encodes mitochondrial ribosomal protein L9 and is required for seed development.

- Plant Physiol 180:2106–2119. https://doi.org/10.1104/pp.19.00546
- Quesada V (2016) The roles of mitochondrial transcription termination factors (MTERFs) in plants. Physiol Plant 157:389–399. https://doi.org/10.1111/ppl.12416
- Quesada V, Ponce MR, Micol JL (1999) OTC and AUL1, two convergent and overlapping genes in the nuclear genome of Arabidopsis thaliana. FEBS Lett 461:101–106. https://doi.org/10.1016/S0014-5793(99)01426-X
- Ramrath DJF, Niemann M, Leibundgut M et al (2018) Evolutionary shift toward protein-based architecture in trypanosomal mitochondrial ribosomes, Science. https://doi.org/10.1126/science.aau7735
- Raschke M, Bürkle L, Müller N, Nunes-Nesi A, Fernie AR, Arigoni D, Fitzpatrick TB (2007) Vitamin B1 biosynthesis in plants requires the essential iron–sulfur cluster protein, THIC. Proc Natl Acad Sci U S A 104:19637–19642. https://doi.org/10.1073/pnas.0709597104
- Robertson WR, Clark K, Young JC, Sussman MR (2004) An *Arabidopsis thaliana* plasma membrane proton pump is essential for pollen development. Genetics 168:1677–1687. https://doi.org/10.1073/pnas.0709597104
- Robles P, Quesada V (2017) Emerging roles of mitochondrial ribosomal proteins in plant development. Int J Mol Sci 18:2595. https://doi.org/10.3390/ijms18122595
- Robles P, Quesada V (2019) Transcriptional and post-transcriptional regulation of organellar gene expression (OGE) and its roles in plant salt tolerance. Int J Mol Sci 20:1056. https://doi.org/10. 3390/ijms20051056
- Robles P, Quesada V (2022) Unveiling the functions of plastid ribosomal proteins in plant development and abiotic stress tolerance. Plant Physiol Biochem 189:35–45. https://doi.org/10.1016/j.plaphy.2022.07.029
- Robles P, Micol JL, Quesada V (2012) Arabidopsis MDA1, a nuclearencoded protein, functions in chloroplast development and abiotic stress responses. PLoS One 7:e42924. https://doi.org/10.1371/ journal.pone.0042924
- Robles P, Micol JL, Quesada V (2015) Mutations in the plant-conserved MTERF9 alter chloroplast gene expression, development and tolerance to abiotic stress in *Arabidopsis thaliana*. Physiol Plant 154:297–313. https://doi.org/10.1111/ppl.12307
- Robles P, Navarro-Cartagena S, Ferrández-Ayela A et al (2018a) The characterization of *Arabidopsis mterf6* mutants reveals a new role for mTERF6 in tolerance to abiotic stress. Int J Mol Sci 19:2388. https://doi.org/10.3390/ijms19082388
- Robles P, Núñez-Delegido E, Ferrández-Ayela A et al (2018b) *Arabidopsis* mTERF6 is required for leaf patterning. Plant Sci 266:117–129. https://doi.org/10.1016/j.plantsci.2017.11.003
- Scarpin MR, Martinez RE, Harper LC, Szakonyi D, Lan T, Mo B, Tang G, Bailey-Serres J, Browning KS, Brunkard JO (2023) An updated nomenclature for plant ribosomal protein genes. Plant Cell 35:640–643. https://doi.org/10.1093/plcell/koac333
- Schneider CA, Rasband WS, Eliceiri KW (2012) NIH Image to ImageJ: 25 years of image analysis. Nat Methods 9:671–675. https://doi. org/10.1038/nmeth.2089
- Shevtsov S, Nevo-Dinur K, Faigon L et al (2018) Control of organelle gene expression by the mitochondrial transcription termination factor mTERF22 in *Arabidopsis thaliana* plants. PLoS One 13:e0201631. https://doi.org/10.1371/journal.pone.0201631
- Skinner DJ, Baker SC, Meister RJ et al (2001) The Arabidopsis HUEL-LENLOS Gene, which is essential for normal ovule development, encodes a mitochondrial ribosomal protein. Plant Cell 13:2719– 2730. https://doi.org/10.1105/tpc.010323
- Soufari H, Waltz F, Parrot C et al (2020) Structure of the mature kinetoplastids mitoribosome and insights into its large subunit biogenesis. Proc Natl Acad Sci 117:29851–29861. https://doi.org/ 10.1073/pnas.2011301117



- Timmis JN, Ayliffe MA, Huang CY, Martin W (2004) Endosymbiotic gene transfer: organelle genomes forge eukaryotic chromosomes. Nat Rev Genet 5:123–135. https://doi.org/10.1038/nrg1271
- Tobiasson V, Amunts A (2020) Ciliate mitoribosome illuminates evolutionary steps of mitochondrial translation. Elife 9:e59264. https://doi.org/10.7554/eLife.59264
- Waltz F, Nguyen T-T, Arrivé M et al (2019) Small is big in *Arabidopsis* mitochondrial ribosome. Nat Plants 5:106–117. https://doi.org/10. 1038/s41477-018-0339-y
- Waltz F, Soufari H, Bochler A et al (2020) Cryo-EM structure of the RNA-rich plant mitochondrial ribosome. Nat Plants 6:377–383. https://doi.org/10.1038/s41477-020-0631-5
- Waltz F, Salinas-Giegé T, Englmeier R et al (2021) How to build a ribosome from RNA fragments in *Chlamydomonas* mitochondria. Nat Commun 12:7176. https://doi.org/10.1038/s41467-021-27200-z
- Wang X, Auwerx J (2017) Systems phytohormone responses to mitochondrial proteotoxic stress. Mol Cell 68:540-551.e5. https://doi. org/10.1016/j.molcel.2017.10.006
- Wang G, Ellendorff U, Kemp B et al (2008) A genome-wide functional investigation into the roles of receptor-like proteins in *Arabidop-sis*. Plant Physiol 147:503–517. https://doi.org/10.1104/pp.108. 119487
- Wobbe L (2020) The molecular function of plant mTERFs as key regulators of organellar gene expression. Plant Cell Physiol 61:2004–2017. https://doi.org/10.1093/pcp/pcaa132
- Xu T, Lee K, Gu L et al (2013) Functional characterization of a plastidspecific ribosomal protein PSRP2 in *Arabidopsis thaliana* under abiotic stress conditions. Plant Physiol Biochem 73:405–411. https://doi.org/10.1016/j.plaphy.2013.10.027
- Yamaguchi-Shinozaki K, Shinozaki K (2006) Transcriptional regulatory networks in cellular responses and tolerance to dehydration

- and cold stresses. Annu Rev Plant Biol 57:781–803. https://doi.org/10.1146/annurev.arplant.57.032905.105444
- Yuan H, Liu D (2012) Functional disruption of the pentatricopeptide protein SLG1 affects mitochondrial RNA editing, plant development, and responses to abiotic stresses in *Arabidopsis*. Plant J 70:432–444. https://doi.org/10.1111/j.1365-313X.2011.04883.x
- Zhang H, Luo M, Day RC et al (2015) Developmentally regulated *HEART STOPPER*, a mitochondrially targeted L18 ribosomal protein gene, is required for cell division, differentiation, and seed development in *Arabidopsis*. J Exp Bot 66:5867–5880. https://doi.org/10.1093/jxb/erv296
- Zhu Q, Dugardeyn J, Zhang C et al (2014) The Arabidopsis thaliana RNA editing factor SLO2, which affects the mitochondrial electron transport chain, participates in multiple stress and hormone responses. Mol Plant 7:290–310. https://doi.org/10.1093/mp/ sst102
- Zsigmond L, Rigó G, Szarka A et al (2008) Arabidopsis PPR40 connects abiotic stress responses to mitochondrial electron transport. Plant Physiol 146:1721–1737. https://doi.org/10.1104/pp.107. 111260
- Zsigmond L, Szepesi Á, Tari I et al (2012) Overexpression of the mitochondrial *PPR40* gene improves salt tolerance in *Arabidopsis*. Plant Sci 182:87–93. https://doi.org/10.1016/j.plantsci.2011.07. 008

Publisher's Note Springer Nature remains neutral with regard to jurisdictional claims in published maps and institutional affiliations.

